

Review

Metal–Organic Frameworks for Electrocatalytic Sensing of Hydrogen Peroxide

Shuhan Wang, Tong Zhang, Xukun Zhu, Shu Zu, Zexin Xie, Xiaoxiang Lu, Mingdao Zhang *, Li Song and Yachao Jin

Jiangsu Key Laboratory of Atmospheric Environment Monitoring and Pollution Control, Jiangsu Collaborative Innovation Center of Atmospheric Environment and Equipment Technology, Institute of Energy Supply Technology for High-End Equipment, School of Environmental Science and Engineering, Nanjing University of Information Science & Technology, Nanjing 210044, China; wsh2638237340@outlook.com (S.W.); zhangtong9696@163.com (T.Z.); xukunzhu7@gmail.com (X.Z.); zushu_zs@163.com (S.Z.); xiezexin2001@163.com (Z.X.); 11214490676@163.com (X.L.); songli@nuist.edu.cn (L.S.); jinyachao@nuist.edu.cn (Y.J.)

* Correspondence: matchlessjimmy@163.com

Abstract: The electrochemical detection of hydrogen peroxide (H_2O_2) has become more and more important in industrial production, daily life, biological process, green energy chemistry, and other fields (especially for the detection of low concentration of H_2O_2). Metal organic frameworks (MOFs) are promising candidates to replace the established H_2O_2 sensors based on precious metals or enzymes. This review summarizes recent advances in MOF-based H_2O_2 electrochemical sensors, including conductive MOFs, MOFs with chemical modifications, MOFs-composites, and MOF derivatives. Finally, the challenges and prospects for the optimization and design of H_2O_2 electrochemical sensors with ultra-low detection limit and long-life are presented.

Keywords: H_2O_2 ; MOFs; electrochemical detection; sensors



Citation: Wang, S.; Zhang, T.; Zhu, X.; Zu, S.; Xie, Z.; Lu, X.; Zhang, M.; Song, L.; Jin, Y. Metal–Organic Frameworks for Electrocatalytic Sensing of Hydrogen Peroxide. *Molecules* **2022**, *27*, 4571. <https://doi.org/10.3390/molecules27144571>

Academic Editor: Wei-Yin Sun

Received: 13 April 2022

Accepted: 7 July 2022

Published: 18 July 2022

Publisher's Note: MDPI stays neutral with regard to jurisdictional claims in published maps and institutional affiliations.



Copyright: © 2022 by the authors. Licensee MDPI, Basel, Switzerland. This article is an open access article distributed under the terms and conditions of the Creative Commons Attribution (CC BY) license (<https://creativecommons.org/licenses/by/4.0/>).

1. Introduction

Hydrogen peroxide (H_2O_2) is an indispensable component in living organisms as a biological intermediary, and has been widely applied as an essential reagent in daily life, industrial fields, medical treatment, and other sections. However, a high concentration of H_2O_2 is corrosive and can cause serious injury when contacts with the skin, and accidental ingestion of H_2O_2 can result in gas embolism in several organs, especially in heart, lung and esophagus [1–4]. The strong oxidizing property of H_2O_2 can even be applied for the preparation of explosives, which may threaten people's lives [5,6]. More importantly, the harm caused by low-concentration H_2O_2 should not be underestimated. Actually, trace amounts of H_2O_2 produced in the cells can cause the induced oxidation of melanocytes, resulting in the death of melanocytes, which is also the main cause of vitiligo [7]. Abnormal production of H_2O_2 in mitochondria can cause reversible mitochondrial swelling, rupture and cellular structural changes, which can induce diseases such as diabetes, Parkinson's diseases and cancers [8]. Therefore, it's of great significance to detect low concentration of H_2O_2 .

For now, a great number of H_2O_2 detection approaches, such as electrochemical detection [9], fluorescence [10], titration [11] and chromatography [12] have been employed in detecting H_2O_2 concentration. However, traditional methods are no longer applicable in many fields with the higher requirements for H_2O_2 detection. For instance, precision data and low detection limit can be obtained through fluorescence detection, while high detection cost and requirement of sample preparation remain a problem [13]. Compared with fluorescence detection method, the colorimetric detection method itself has the advantages of low cost and fast detection speed. However, the raw materials can be easily

denatured which makes it difficult to prepare [14]. In contrast, electrochemical detection method has been widely used owing to its advantages of simplicity, rapidity, sensitivity and economy [15,16]. Despite that, electrochemical H_2O_2 detection usually requires a higher potential for direct reduction or oxidation on the surface of the bare electrode, resulting in a less current response. Therefore, it is essential to improve the bare electrode or design new electrode materials to increase the sensitivity of the H_2O_2 sensor and speed up the response time for the detection of ultra-low concentration of H_2O_2 [17].

2. Research Status and Challenges

Hitherto, various strategies have been reported to modify the electrodes. Among them, the most common one is to prepare the metal oxide modified electrodes. It has been observed that the electrocatalytic materials containing Fe_2O_3 show excellent catalytic performance, where the detection limit reaches 5 nmol, and they can be applied to detect H_2O_2 both inside and outside the cells [18–20]. Apart from Fe_2O_3 , Cu_2O features high specific surface area, good electrochemical activity and the potential to promote electron transfer reactions at a lower overpotential, making it a favorable material for the development of H_2O_2 sensors. Nevertheless, the catalytic activity is affected by the particle size and the shape of the metal oxides. On the whole, the large particle size and irregular morphology reduce the effective contact between the catalytic materials and the H_2O_2 molecules, resulting in incomplete catalytic activity and reduced catalytic effect [21,22]. Additionally, enzymes are often used to modify the electrodes due to their perfect selectivity for H_2O_2 . Horseradish peroxidase (HRP), as one of the most common H_2O_2 enzymes, although has been extensively studied and used for manufacturing H_2O_2 sensors [23], its application has been restricted by the complex immobilization process and the instability during the detection [24]. Currently, precious metal nanoparticles (Pt, Ag, Ru et al.) have been widely implemented in H_2O_2 detection technology due to their unique electronic structure, prominent physical and chemical properties [25]. For instance, AuNCs (nanoclusters) is an emerging nanomaterial that exhibits excellent performance and can improve the sensitivity of H_2O_2 detection [26]. B. Patella and co-workers designed the rGO/Au-NPs (nanoparticles)-based electrode through a three-electrode deposition method to monitor H_2O_2 released by the human macrophages [27]. However, considering the scarcity of precious metals, it is necessary to find and develop new materials with low cost and high catalytic activity to replace precious metals [28,29].

In recent years, numerous new materials have also been used for electrochemical detection of H_2O_2 , such as CNTs (carbon nanotube), graphene and metal organic frameworks (MOFs) [30–32]. As we know, the electrical conductivity and catalytic performance can be improved by the carbon coating method; when the graphene oxide nanoflake is covered by nano-scale graphene, the subsequently synthesized graphene oxide/graphene composite material presents a better performance on H_2O_2 detection with high catalytic activity and electrochemical stability [33]. Yu et al. [34] developed a novel/graphene (NiO/GR) nanocomposite that exhibited high sensitivity to H_2O_2 , the GR coating improved the electrochemical stability and its anti-interference ability. MOFs have drawn increasing interest and been applied to gas storage/separation [35–44], drug delivery [35–44], energy storage/conversion [35–44] and multiphase catalysis [35–44] due to their tunable pore sizes, diverse structures, and abundant functional designs [35–44]. Moreover, the ordered arrangement of metal sites and organic ligands provide abundance of accessible catalytic sites and confer intrinsic enzyme-mimetic properties to MOFs compared to other types of nanozymes [45]. For example, Zhang [46] developed the new class of 2D conductive MOFs films $[\text{Co}_3(\text{HHTP})_2]_n$ by LB (langmuir-blodgett) technology. The porous structures and exposed Co active sites from the $[\text{Co}_3(\text{HHTP})_2]_n$ had superior catalytic activity for H_2O_2 . In addition, some MOFs with mesh structures can be used as carriers for other materials to form composite materials with new functions [46]. There have been several review reports on the use of MOFs for H_2O_2 sensors [45,47–52], for example, Li et al. [45,47–52] classified MOFs into four categories and reviewed the progress of MOFs in chemical sensors, includ-

ing the detection of H₂O₂. Goncalves et al. [45,47–52] reviewed the development of MOFs derivatives for sensors. However, most of these reports are not comprehensive enough to introduce all of the types of MOFs-based H₂O₂ sensors. What's more, instead of focusing on H₂O₂ detection, variety of molecules are also included, which makes most of these reviews not deeply explore the mechanism of MOFs for H₂O₂ sensing, as well as the design and development of MOFs H₂O₂ electrochemical sensors. In this paper, based on the reviews of the same topic, as well as the latest research progress, we found that MOFs can exert more structural advantages in electrochemical detection of H₂O₂ (strong adsorption, faster electron transport, and high conductivity) and become more competitive as a sensor. Here, we deeply explore the detection mechanism of electrochemical H₂O₂ for different types of MOFs, some bright ideas for the design and improvement of MOFs-based electrochemical H₂O₂ sensors are proposed based on the recent research progress. Firstly, the sensing mechanism and working principle of MOFs-based H₂O₂ electrochemical sensors are distinctly introduced. Secondly, as shown in Figure 1, we categorize the recent reported MOFs-based H₂O₂ electrochemical sensors as: (1) conductive MOFs based H₂O₂ sensors; (2) chemically modified MOFs based H₂O₂ sensors; (3) MOFs composites based H₂O₂ sensor; (4) MOF derivatives based H₂O₂ sensors. Finally, problems and trends for future MOFs-based H₂O₂ electrochemical sensors are discussed. We hope that our perspectives will be useful for future development of advanced MOF-based H₂O₂ sensors. In addition, the performance of recently reported MOFs-based H₂O₂ electrochemical sensors are shown in Table 1. We also summarized the following characteristics as the keys to develop MOFs-based H₂O₂ electrochemical sensors with excellent performance:

(i) Conductivity

High electrical conductivity is vital to electron transfer in the process of H₂O₂ splitting. In general, the electrical conductivity of MOFs depends on the carrier mobility and internal charge density. The π -conjugated structure forms a continuous conductive network to facilitate the conduction of electrons. In addition, high-energy electrons or holes in metal ions can induce high concentrations of loosely bound carriers, thereby increasing the charge density. The direct connection between the metal nodes and the organic ligands can effectively reduce the energy mismatches and further promote the charge delocalization and electron transfer.

(ii) Activity

The catalyst activity is an important factor in the decomposition rate of H₂O₂. It is mainly related to the intrinsic catalytic ability and the number of active sites of the catalyst. Generally, the porous structure can not only increase the specific surface area, but also expose more active sites to improve the catalytic activity, thus further improve the adsorption capacity, reduce the activation energy of the intermediate product transformation.

(iii) Selectivity

An ideal electrochemical sensor for H₂O₂ should have high selectivity. For example, H₂O₂ samples may be mixed with other substances (glucose, ascorbic acid, ethanol, etc.), and they will also undergo redox reactions. Therefore, the sensors should only respond to H₂O₂ at a specific voltage.

(iv) Stability

The commercial H₂O₂ electrochemical sensors must possess excellent chemical and structural stability in hostile acidic and alkaline environments. In specific cases, it may suffer from changes in catalyst structure and reduced catalytic activity due to the particle agglomeration during the long-time detection process. Therefore, in order to ensure the accuracy of the test, especially in medical clinical applications, the requirement of high stability need be met in the design of commercialized sensors.

(v) Low-cost

Precious metal electrocatalysts (e.g., Pt, Au, Ag, Pd) have high catalytic activity, but their scale-up application is limited by high cost, limited reserves, poor stability, low sensitivity and selectivity. Alternatively, MOFs-based catalysts are commonly ligated with transition metals, which have inherently good catalytic activity and can be feasibly prepared by simple methods (hydrothermal method, ultrasonic method et al.). Thus, in order to meet the goal of commercial development, the raw materials and preparation methods of the H_2O_2 electrochemical sensors should follow the principles of low cost and low time consumption.

(vi) Environmental-friendly

The concept of low-carbon green development is of great significance to the sustainable development of human society. Specifically, the raw materials for the H_2O_2 electrochemical sensors should be non-toxic and non-polluting. The preparation process should not produce hazardous gases and solutions. What's more, the catalysts must be non-hazardous to the cells, in order to meet the medical detection requirements.

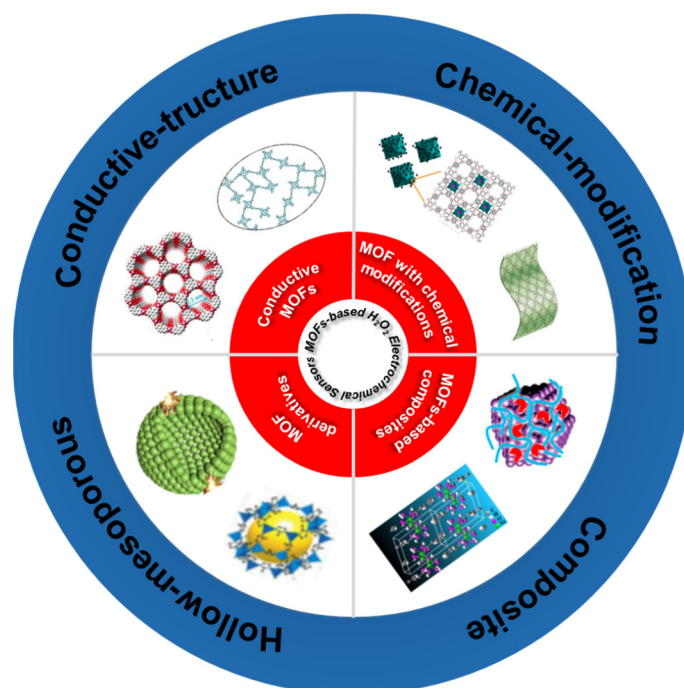


Figure 1. Conductive MOFs based H_2O_2 sensors; chemically modified MOFs-based H_2O_2 sensors; MOFs composites based H_2O_2 sensor; MOF derivatives based H_2O_2 sensor.

Table 1. Recently reports of H₂O₂ electrochemical sensors.

Electrochemical Sensor	Electrolyte	Detection Limit (μM)	Linear Range	Practical Application	Reference
Conductive MOFs based H₂O₂ sensors					
[Co ₃ (HHTP) ₂] _n	0.1 M NaOH	2.9	-	-	[2]
[Co ₃ (HOB) ₂] _n	0.1 M NaOH	0.00308	-	-	[36]
[Cu(adp)(BIB)(H ₂ O)] _n /GC	0.1 M KOH	0.068	0.1 μM–2.75 μM		[53]
2D Co-MOF	0.1 M KOH	0.69	0.5 μM–832.5 μM		[54]
FePc-CP NSs	0.1 M PBS	0.017	0.1–1000 μM	A549 live cells, Orange juice and beer	[55]
Co-MOF/TM	0.1 M PBS	0.25	1–13,000 μM	A549 cells	[56]
CuMOFs@FeP-pSC ₄ -AuNPs	10 mM PBS	47	0.5–2.5 mM	Cancer cells	[57]
NENU5	0.1 M PBS	1.03	10–50,000 μM	-	[58]
CuCo-BDC/GO	0.1 M PBS	0.069	100 nM–3.5 mM	Human serum samples	[59]
HKUST-1/GCE	0.1 M PBS	0.68	2 μM–3 Mm and 3–25 mM	Milk sample	[60]
MOF composites based H₂O₂ sensors					
MIL-53-CrIIIAS/GCE	0.1 M NaOH	3.52	25–500 mM,	-	[54]
Ni(II)-MOF/CNTs nanocomposites	0.1 M NaOH	2.1	0.01–51.6 mM		[61]
MNPs@Y-1, 4-NDC-MOF/ERGO	0.1 M PBS	0.18	4–11,000 μM	A549 cells	[62]
Ni-MOF nanosheets/Hemin	0.1 M PBS	0.2	1–400	Human serum samples	[9]
GCE/GO/poly(CoTBIPc)	0.1 M PBS	0.6	2–200 μM	-	[3]
A-Ni ₁ Mo _{0.5} -MOFs@AAC	PSB	0.185	-	-	[63]
CuCo-BDC/GO	0.1 M PBS	0.069	100 nM -3.5 mM	Diluted human serums	[59]
CuMOF/MXene/GCE	0.1 M PBS	0.35	1 μM–6.12 mM	Serum	[64]
Cu-TCPP MOF/Cu _{5,4} O	0.1 M PBS	0.13	0.0001- 0.59 mM and 1.59–20.59 mM	Living cells	[65]
Cu-MOF@S-Gr	0.1 M PBS	0.0113 ± 0.00004	0.1–3 μM	Tap water	[66]
Au-Pd@UiO-66-on-ZIF-L/CC	0.01 M PBS	0.0212	1 μM–19.6 mM	A549 cells	[67]
Cu@BDC(NH ₂)@2-MI	0.1 M PBS	0.97	10 μM–13.28 mM		[68]
MnO _x	0.2 M PBS	0.000232	0.000696–742 μM	Human serum and milk sample	[69]
NCNT MOF CoCu	0.1 M PBS	0.206	0.05–3.5 mM	Serum samples	[70]
Ag-Bi BDC (s) MOF/GCE	0.1 M PBS	0.020.1	10 μM–5 mM and 5 mM–145 mM	THP-1 and AtT-20 cancer cells	[71]
MOF derivatives based H₂O₂ sensors					
AuPt/ZIF-8-rGO	0.1 M PBS	0.019	0.1–18,000 μM	Human serum	[72]
MOF-Au@Pt nanoflowers	PBS	0.086	0.8 μM–3 mM	Suspension of living cell	[32]
Co-NC RDCs	0.1 M PBS	0.143	0.001–30 mM		[73]
MIL-101(Fe)@Fe ₃ O ₄ /NGCE	0.1 M PBS	0.15	0.001–0.01 mM	Human blood plasma	[74]
Co (4%)–N/CNS	0.4 M PB	0.00618	1–500 μM and 500 μM–0.1 M	Human serum	[75]
Co-NPs/NCs	0.01 M PBS	0.12	10–2080 μM and 2080–11,800 μM	Human serum sample	[76]
Cu-MoO ₂ -C	PBS	0.16	0.25–6.25 mM		[77]
ZnO@ZIF-8	0.1 M PBS	3	20–11,550 μM		[78]
Co ₃ O ₄ @CNBs	0.01 M PBS	0.00232	10 nM–359 μM	HUVEC cells and 4T1, A549 cancer cells	[79]

3. Sensing Mechanisms and Working Principles of MOFs-Based H₂O₂ Electrochemical Sensor

3.1. Electrochemical Sensor Detection Principle

Generally, the electrochemical detection of H₂O₂ is achieved by applying a corresponding voltage to the electrochemical sensor, followed by the oxidation or reduction of H₂O₂ on the electrode surface. The electric charges of the redox process are captured by the electrode and converted into an electrochemical signal. Qualitative and quantitative analysis of H₂O₂ can be obtained through the change in the peak voltage and current. The schematic diagram of electrochemical detection of H₂O₂ is shown in Figure 2. Commonly, H₂O₂ detection is performed under neutral or alkaline conditions, with certain differences in the reaction mechanism. Specifically, the difference lies in whether the catalyst produces a reducing or oxidizing effect on H₂O₂ during the detection: if the catalyst appears in an oxidized state, the H₂O₂ is oxidized; and if the catalyst is in a reduced state, the H₂O₂ is reduced. We will discuss the specific steps of H₂O₂ catalytic decomposition in the following sections.

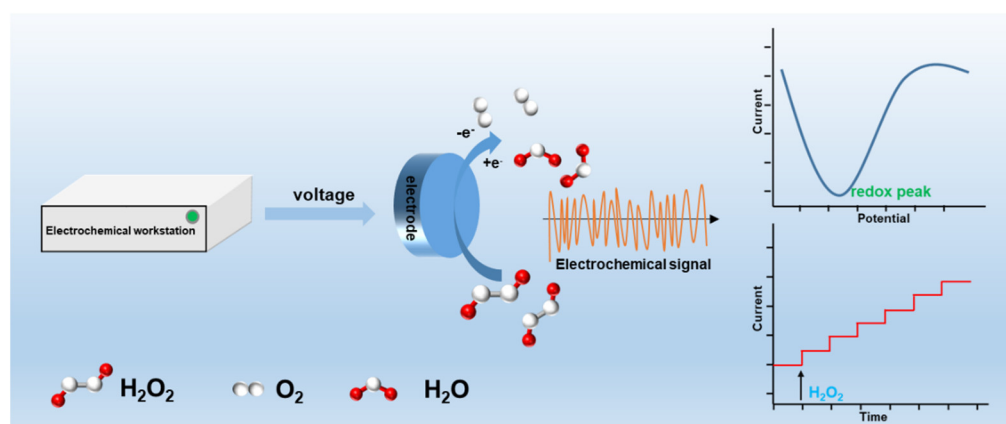
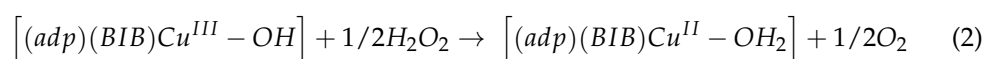
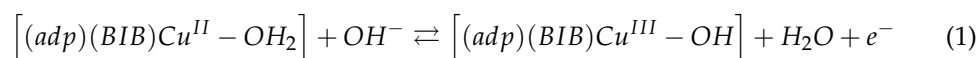


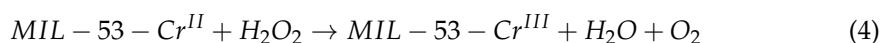
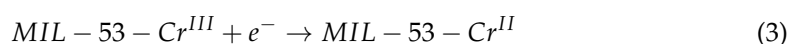
Figure 2. Schematic diagram of H₂O₂ detection by electrochemical sensor.

3.2. Detecting under Alkaline Condition

Under alkaline conditions, the catalytic decomposition of H₂O₂ mainly depends on the redox changes of metal sites. In the first case, the catalyst combines with OH[−] to form intermediates with higher valence state of the metal sites and electrons, then the intermediates react with H₂O₂ to return to the original valence state, and H₂O₂ is decomposed. The mechanism can be illustrated by the following equation [80]:



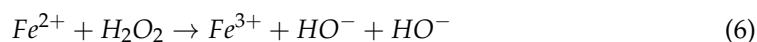
The other situation is that H₂O₂ is adsorbed by catalysts, then the catalysts are reduced as the cathode. After that, the pre-adsorbed H₂O₂ is decomposed by electron transfer with the catalyst. The mechanism can be illustrated by the following equation [80]:



3.3. Detecting under Neutral Condition

It has been reported that the catalytic decomposition of H₂O₂ occurs in the presence of ferrous (Fe²⁺) and ferric (Fe³⁺) ions. The generation of reactive hydroxyl radicals (HO·) is based on the classical Haber Weiss mechanism/Fenton-type reaction [81–84]. The results show that ferrous ions have better catalytic decomposition activity for H₂O₂ in the pH

range of 3–4, while ferric ions have better catalytic activity at a neutral pH. The reactivity study of ferric ions show that the coordinated ferrous ions catalyze the decomposition of H_2O_2 more effectively than the free ferric ions at the neutral pH [82]. In this case, the ferric ions are first reduced into ferrous, and then the ferrous ions are oxidized by H_2O_2 to turn to ferric ions. The electrochemical mechanism of general Fe-MOFs based materials in neutral media are as follows [85]:



4. Design and Synthesis of MOFs Based H_2O_2 Sensor

MOFs are a kind of porous polymer materials connected by metal ions through organic bridge ligands, which combine the advantages of inorganic, organic porous materials and porous hybrids [86–89]. The structural diversity makes some MOFs possess the multi-channel structures which can enhance the electrolyte transport capacity and further increase the electrical conductivity. Furthermore, the reactants can be easily trapped and adsorbed by various active sites and high specific surface areas, thus the conversion of the reaction is facilitated [90]. Therefore, MOFs have great prospect for the preparation of H_2O_2 sensors. In the following sections, some reliable ideas to flexibly apply MOFs materials to the design of H_2O_2 sensors are expounded.

4.1. Conductive MOFs Based H_2O_2 Sensor

Ionic conduction and electron conduction occur along with the H_2O_2 decomposition in the process of detection. However, the conversion efficiency between electrical and chemical energy will be reduced if the conductive orbit cannot be effectively constructed, and leading to decreasing adsorption and catalytic capacity [91]. In general, the formation of conductive network requires coordination interaction between metal ions and organic ligands. Ligands with π -conjugated structures can form a continuous conductive network to facilitate electron conduction. High concentration of loose carriers formed by high-energy electrons or holes in metal ions can increase charge density [91]. The direct connection between metal nodes and organic ligands (such as N, O, S-based ligands) can effectively reduce the energy mismatch, further promoting the charge delocalization and electron transport [92–94]. Based on the charge transfer mode, the conductive mechanism of conductive MOFs can be divided into three types as follow: charge transfer “through space”, through-bond conduction and through-guest conduction [95].

Aromatic hydrocarbons are a class of compounds with conjugated structures, such as 2,3,6,7,10,11-hexaiminotriphenylene (HITP), 2,3,6,7,10,11-hexahydroxytriphenylene (HHTP) and benzenehexol (HOB). These π -conjugated aromatic systems are capable of cooperating with metal nodes to dominate the conduction process. The π - π interaction between the systems and metals facilitates both “through-bond” and “through-space” electronic conduction [96,97]. Our group [36] designed the 2D $[Co_3(HOB)_2]_n$ conductive MOF nanosheets with abundant nanoscale channels. HOB and Co^{2+} ions were coordinated at the water-air interface to form a single-layer nanosheets with high structural order through LB method (Figure 3a). $[Co_3(HOB)_2]_n$ nanosheets were arranged in a long-range order, and then the π - π stacks in the internal pores were formed by original growth on the FTO (fluorine-doped tin oxide) glass. Meanwhile, the coordination of Co-O reduced the energy mismatch, facilitated the charge delocalization and electron transport. The counterion pair generated from electrostatic interactions leads to the feasible electronic adjustment and migration [98,99]. More importantly, the porous structure for proton transport and the exposed metal sites equip the 3-layer nanosheets with excellent reducibility to H_2O_2 with a LOD (limit of detection) of 3.08 nM (Figure 3b), and it possesses the lowest detection limitation among the current non-precious metal conductive MOFs based H_2O_2 sensors. It could also be

concluded that the common drugs and ion concentration had no impact on H_2O_2 detection. Noticeably, the activity of $[\text{Co}_3(\text{HOB})_2]_n$ exhibited almost no attenuation after 1000 CV cycles (Figure 3c). Park [80] et al. reported a Co-based 2D conductive MOF, Co-HAB. The high conductivity (1.57 S cm^{-1}), porosity and high density of redox active sites of Co-HAB provided a possibility for ion storage and energy conversion, which may improve the catalytic activity when used for H_2O_2 reduction. At the same time, excellent chemical and thermal stability increase the utility of sensors. This offers a bright future for the preparation of H_2O_2 sensors with low detection limit.

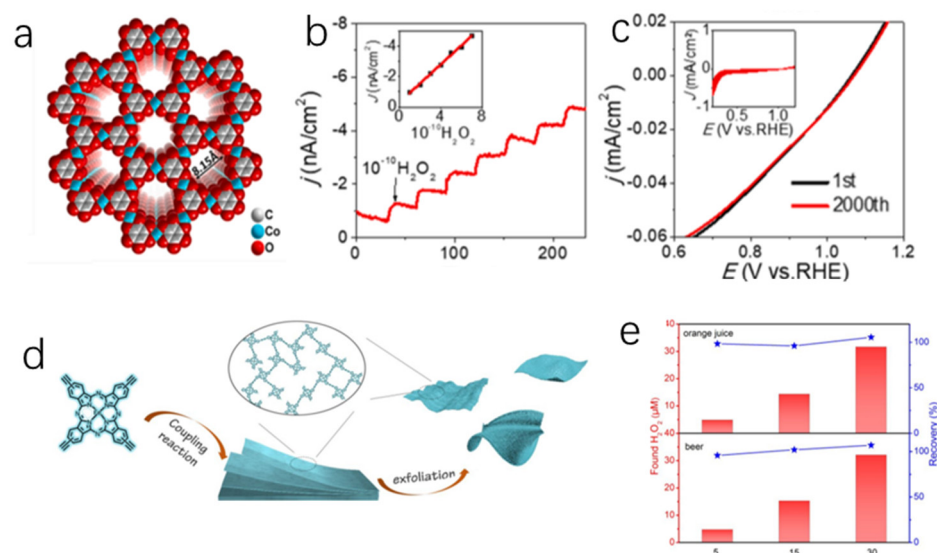


Figure 3. (a) The space-filling model of $[\text{Co}_3(\text{HOB})_2]_n$; (b) H_2O_2 injection responses of the current density of 3-layer $[\text{Co}_3(\text{HOB})_2]_n$ films (The inset shows the linear relationship between the current density and the injected H_2O_2 amount.); (c) Tolerance of regular species. LSV curves before/after 1000 CV cycles. (The inset shows the 1000-cycle CV curves.) [36]; Copyright 2021, Elsevier. (d) Schematic diagram for the synthesis of the FePc-CP NSs; (e) Determination of H_2O_2 in commercial orange juice and beer [55]. Copyright 2019, ACS.

Coordination bonds composed of metals and organic ligands with matched energy levels and good orbital overlap can generate long-distance charges transfer path, which is beneficial for improving the charge transfer [100]. Liu [55] reported an advanced FePc (iron phthalocyanine) -based diyne-linked ($-\text{C}\equiv\text{C}-\text{C}\equiv\text{C}-$) conjugated polymers 2D NSs (nanosheets) (FePc-CP NSs) (Figure 3d). It has been demonstrated that the high reduction activity of the catalyst for H_2O_2 detection (LOD was $0.017 \mu\text{M}$) is mainly attributed to the following points: (1) FePc is beneficial to promote the cleavage of O-O bonds between O_2 and peroxide and thereby accelerates the decomposition of H_2O_2 ; (2) diyne-linked ($-\text{C}\equiv\text{C}-\text{C}\equiv\text{C}-$) conjugated structure enhances the conductivity; (3) highly exposed heme-like active centers in layered pore junctions increase catalytic activity. FePc-CP NSs accurately detected H_2O_2 in beer and orange juice with a recovery of 95.8~107% (Figure 3e), this showed that the FePc-CP NSs had the potential to detect the H_2O_2 in food. Since then, we can conclude that long-range ordered nanochannels formed by the accumulation of 2D π -conjugates can realize the electrolyte transport. This approach to creating the charge transport by using covalent bonds of extended coordination polymers in porous frameworks provides a unique platform for the development of high sensitive H_2O_2 sensors.

Apart from the above mentioned, improving the concentration of proton carriers is a key factor to construct highly conductive and stable MOFs. The most effective strategy is to introduce the Lewis acid particles [101,102], molecules or counter ions [103,104] and the incorporation of proton-related substituents ($-\text{NH}_2$, $-\text{SO}_3\text{H}$, $-\text{COOH}$, $-\text{OH}$, $-\text{SH}$, etc.) in the ligands [105,106]. The increasing number of these guest molecules and proton carriers will form a hydrogen bonding network and enhance the conductivity [107,108]. Zhang [109]

and coworkers bridged Cu^{2+} with BIB and adp^{2-} to form a 2D propagation network with channel structure. The 2D layer channel structure was further connected by the hydrogen-bond interactions, and then a 3D supramolecular architecture ($[\text{Cu}(\text{adp})(\text{BIB})(\text{H}_2\text{O})]_n$) was formed. $[\text{Cu}(\text{adp})(\text{BIB})(\text{H}_2\text{O})]_n$ performed a high reduction for H_2O_2 with a low LOD (0.068 μM) and an excellent linear range (0.1 μM to 2.75 μM), which could be attributed to the electronic transport effect. Throughout the redox reaction, the channels and hydrogen-bond acted as transport corridors. Protons and electrons were transferred in an ordered manner. Consequently, the adsorption energy of the active sites for electrolytes and intermediates was decreased. Judging from the electron transfer, it was a two-step reaction. Firstly, $[\text{Cu}(\text{adp})(\text{BIB})(\text{H}_2\text{O})]_n$ reacts with OH^- and then Cu^{2+} is oxidized to Cu^{3+} ; secondly, H_2O_2 molecules react with Cu^{3+} and then they are reduced to form O_2 due to the strong oxidizing from Cu^{3+} .

Conductive electrical system consisted of metal ions and ligands with π -conjugate structure solve the serious poor conductivity issue for H_2O_2 electrocatalysts; furthermore, the porous structure is conducive to promoting the mass transfer, and improving the catalytic rate of H_2O_2 decomposition. Still, the high price of organic ligands remains a large obstruction on the pathway to large-scale commercialization.

4.2. Chemically Modified MOFs Based H_2O_2 Sensor

Chemical modification is a feasible and effective way to introduce desired functions into MOFs materials. In general, MOFs can be functionally modified by their metal sites and/or organic linkers. For example, through the hybridization with conducting polymers, the electrical conductivity of the material can be improved [45,110].

Combining MOFs with conductive species can improve electronic conductivity, catalytic activity, and expand applications. The most common method is to combine the active component with carbon-based materials such as carbon nanotubes and ketone black carbon [111]. POMs (polyoxometalates), with internal unconventional molecular structure, stable physical/chemical properties and redox state, have shown superb activity in fabricating electrocatalysis. When they are used to prepare MOFs, the latest material POM-based MOFs (POMOFs) performed high specific surface and exposed more active sites [29,112,113]. However, the low conductivity reduces the catalytic activity of POMOFs as catalysts, resulting in low sensitivity and high detection limits when applied for H_2O_2 detection. Wang et al. [58] developed POM-based MOF (NENU5 (polyoxometalate-based metal-organic framework)) grown in situ on KB by adopting a facile and feasible one-step solution method (Figure 4a). The low detection limit (1.03 μM) of NENU5-KB-3 for H_2O_2 is mainly attributed to the high conductivity of KB and the high catalytic activity of NENU5. It also had a wide linear range from 10 μM to 50 mM and a high sensitivity of 33.77 $\mu\text{A mM}^{-1}$. More notably, the residual current decreased by ~9% after continuous testing in 30 μM H_2O_2 for 4 h. It indicated NENU5-KB-3 had good structural stability and stable catalytic activity. Furthermore, drug resistance results have revealed that the successive addition of 0.2 mM AA, 0.2 mM APAP, 0.2 mM DA and 0.2 mM glucose exerted no influence on H_2O_2 detection, representing excellent stability and high selectivity.

Conductive substrates such as carbon cloth, FTO, ITO [112–114], etc. are also often used as supports for MOFs. They can improve the conductivity while exposing more active components, greatly improving the catalytic activity. Xia [56] and coworkers synthesized Co-MOF nanosheets array supported on Ti mesh (Co-MOF/TM). Co-MOF was synthesized by coordination of Co^{2+} with terephthalic acid. With notable properties of large surface area, good stability, high porosity, and rich unsaturated Co^{2+} sites, Co-MOF/TM exhibited outstanding catalytic performance with a low detection limit (0.25 μM). The catalytic activity can be attributed to the appearance of electronic defects on the surface of the nanosheets arising from the interaction between the Ti lattices and the Co-MOF. The sensor also showed good utility for monitoring the release of H_2O_2 from A495 cells. Compared with most MOFs, Co-MOF had a lower cost in both raw materials and the preparation process.

The prospective availability of free space in MOFs permits another method of inducing conductivity, namely the introduction of guests (electron donors or acceptors). In some cases, they are complementary to the charge transfer of MOFs junctions or nodes. This approach not only enables the manufacture of conductive MOFs, but also allows their conductive properties to be modulated by specific stimuli without destroying their structure [95]. Hu et al. [57] assembled the petal-like nanonetwork structures by embedding the combination of pSC₄-AuNPs and FeP on the surface of CuMOFs (Figure 4b). On the basis of maintaining the original catalytic activity, selective functionalization and well-defined configurations of CuMOFs, FeP (guest) and pSC₄-AuNPs (body) were interlinked to form a nanonetwork structure for synergistic electron transfer to overcome the drawback of poor conductivity. The dual metallic active sites from the CuMOFs@FeP-pSC₄-AuNPs increased the peroxidase activity, electrocatalytic activity and provided good thermal and storage stability. From which, it realized specific recognition of cancer cells by the signal output from the electronic transfer generated of H₂O₂ decomposition, providing potential applications for clinical cancer detection (Figure 4c).

Transition metal elements are crucial components to build active adsorption sites in MOFs structures. Among them, Ni, Co and Fe show high activity in the kinetics of H₂O₂ decomposition [53,115]. Ni ion has become an important non-precious metal ion for the detection of H₂O₂, and the substantial coordination number makes it easy to coordinate with organic ligands [116]. It is worth noting that the dispersion of unsaturated metal sites in MOFs plays an important role in the kinetic activity of H₂O₂ decomposition [117]. Therefore, the introduction of another metal can produce more active sites to improve the electrochemical properties. In general, the synergistic interaction of two or more substances effectively improves electrocatalytic performance. This optimizes the electronic structure, reduces kinetic barriers and improves the charge transfer between the host metal atoms and the dopants during catalysis [118–120]. Li et al. [63] reported a new bimetallic MOF (A(B)-Ni₁Mo_{0.5}-MOFs@AAC) by the liquid-phase and hydrothermal methods. Mo exhibited a strong hydrogen binding capacity and had a higher activity in the decomposition of H₂O₂ [121]. What's more, the introduction of Ni-Mo bimetallics enhanced the stability of the frameworks, and contributed to the catalytic performance (Figure 4e). Therefore, the A(B)-Ni₁Mo_{0.5}-MOFs@AAC exhibited an outstanding detection performance for H₂O₂ with a high sensitivity (0.277 μA μM⁻¹) and a noteworthy low detection limit of 0.185 μM. The establishment of bimetallic MOFs offers a new and simple idea for designing H₂O₂ sensors with high structural stability and excellent catalytic activity.

Today, widely reported MOFs such as MIL (materials of institut lavoisier)-53(Fe), Fe-NH₂-MIL-88, MIL-68(Fe), and MIL-100(Fe), etc. all exhibit salient H₂O₂ decomposition properties. The narrow pore channels from the 3D block crystal structure restrict the diffusion rate of the substrate, and they further reduce the accessible active site in the 3D native crystal [46,122]. The special structure of 2D nanomaterials, such as large specific surface area, thin thickness and high surface volume, can expose more active sites on the surfaces, thus reducing the mass transfer resistance and diffusion potential barrier [123–126]. Wang et al. [127] synthesized a 2D bimetallic MOF nanosheets (2D Co-TCPP (tris (1-chloro-2-propyl) phosphate) (Fe)) with a thickness of less than 10 nm for the first time through a surface activity-assisted approach (Figure 4f). The highly exposed active sites enabled 2D Co-TCPP(Fe) to exhibit excellent H₂O₂ catalytic decomposition activity with a detection limit of 0.15×10^{-6} M. In addition, the sensor was successfully used for the real-time monitoring of H₂O₂ secreted by living cells. The synthesis of 2D Co-TCPP(Fe) offers a versatile method for developing 2D bimetallic MOF nanosheets in high yields, which can be applied to a variety of areas.

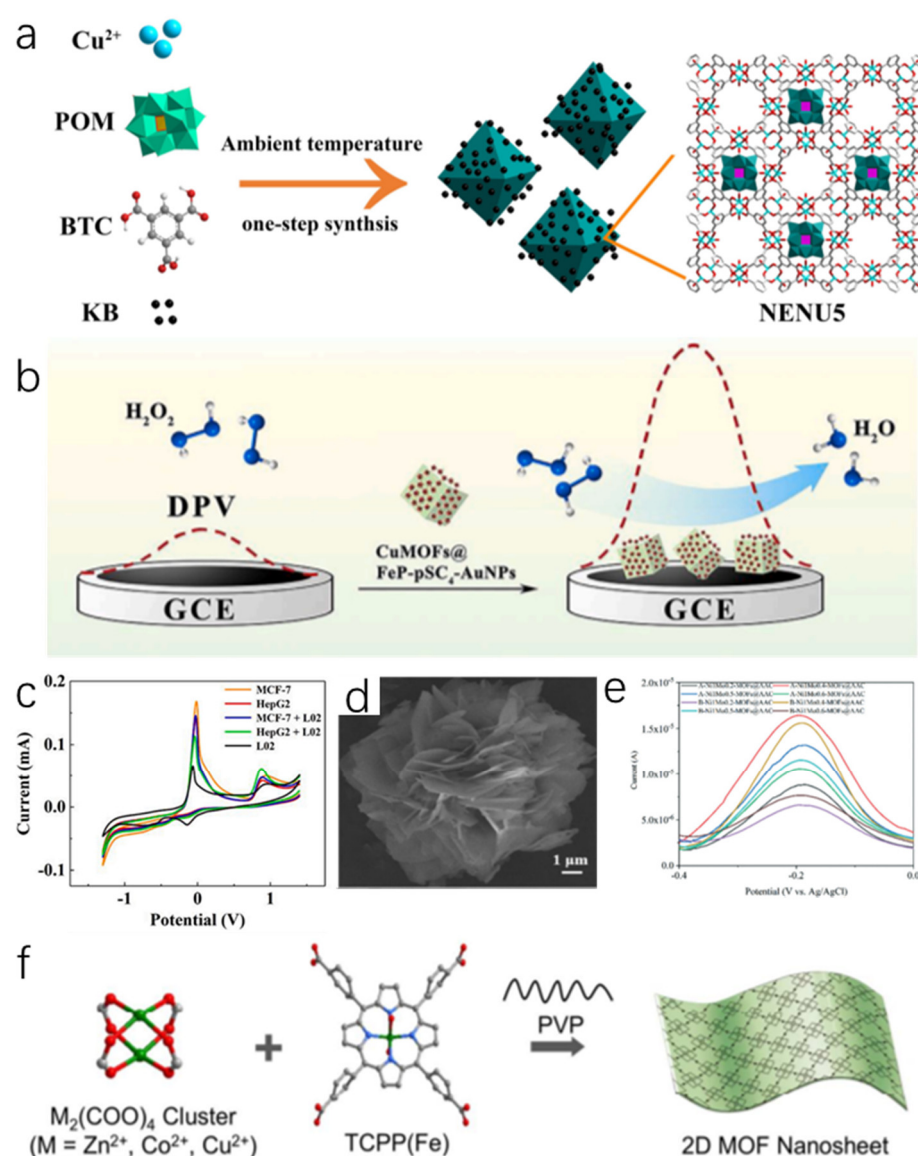


Figure 4. (a) Schematic illustration of the synthesis procedure for NENU5-KB composites [58]; Copyright 2018, Wiley. (b) Schematic illustration of the electrocatalytic reaction of H_2O_2 catalyzed by CuMOFs@FeP-pSC₄-AuNPs; (c) CV responses of H_2O_2 with different cells [57]; Copyright 2021, Elsevier. (d) SEM image of Ni-MOFs [9]; Copyright 2019, Elsevier. (e) DPV curves of A(B)-Ni_xMo_y-MOFs@AAC sensors [63]; Copyright 2020, Royal Society of Chemistry. (f) Scheme showing the surfactant-assisted bottom-up synthesis of 2D MOF nanosheets [127]. Copyright 2017, ACS.

4.3. MOF Composites Based H_2O_2 Sensor

Metal nanoparticles are a kind of economic, stable, simple to prepare nanomaterials, which have similar enzyme action to specific molecules [128,129]. In particular, “d” electron orbitals of precious metal nanomaterials are not filled, the surface may become easier to adsorb reactants. The moderate strength facilitates the formation of intermediate “active compounds” with high catalytic activity and excellent properties such as high temperature resistance, oxidation resistance and corrosion resistance [130,131]. Moreover, the active sites on their surface give them properties similar to those of biological enzymes [128,129]. Since MOFs have a permanent porous structure, the advantages of nanoparticles and MOFs can be utilized by introducing specific nanoparticles into MOFs to form a more stable material [132]. Shazia et al. [67] obtained a bimetallic MOF (Au-Pd@UiO-66-on-ZIF (zeolite imidazolium ester skeleton structure material) -L/CC) by introducing Au nanoparticles into Pd@UiO-66-on-ZIF-L/CC (Figure 5a). Electrochemical test results showed that the

introduction of Au nanoparticles increased the adsorption sites of H_2O_2 , and the synergistic effect between Au nanoparticles and Pd improved the catalytic performance (LOD was 21.2 nM), anti-interference, reproducibility, repeatability and stability of H_2O_2 sensor. Meanwhile, real-time in situ detection of H_2O_2 was achieved by culture of human adenocarcinoma alveolar basal epithelial cells (A549 cells) on Au-Pd@UiO-66-on-ZIF-L/CC, suggesting that the sensor has potential applications in cancer pathology (Figure 5b,c). Li et al. [62] prepared MNPs (magnetic nanoparticles) @Y-1, 4-NDC-MOF/ERGO (M = Ag, Cu) ternary composites by cation exchange strategy and electrochemical reduction. The embedding of metal nanomaterials improved the catalytic activity of the material, while the fast electron transfer effect of ERGO increased the electrical conductivity. What's more, the size tunability and selectivity (Figure 5d,e) of MOFs provided the material with high selectivity to H_2O_2 . The material had potential applications in detecting the release of H_2O_2 from cells. The interaction between the active component and the supporter plays a pivotal role in the catalytic reaction. On the one hand, uniform dispersion of metal nanoparticles can effectively increase the specific surface area while the unity of metal nanoparticles will minimize the specific surface area and surface energy, resulting in a severe loss of structural properties [131]. In order to increase the catalytic activity by loading more metallic nanoparticles, suitable carriers (crystals with high chemical stability, large specific surface area and high porosity) are preferably selected to disperse and immobilize metal particles [133,134]. Based on the large specific surface area, sufficient pore capacity and excellent crystallinity of MOF-67, Wang et al. [32] uniformly dispersed Au@Pt bimetallic nanoflowers on its surface. Compared with the single metal materials, Au@Pt with core-shell structure of bimetallic nanoflowers showed abundant active sites, good electrical conductivity, and better H_2O_2 catalytic activity. The large specific surface area of the MOFs material provides more loading sites for more nanoparticles, thus further enhancing the catalytic effect. They have been proven to be a powerful electrochemical sensing platform with promising applications in biomedical monitoring and environmental analysis. In addition, some researchers have improved electrocatalytic performance by combining MOFs with 2D materials such as graphene or black phosphorus nanosheets to form novel composites. Cheng et al. [64] combined Mxene with MOFs to form a new 3D flower-like Cu-MOF/Mxene/GCE (glassy carbon electrode) material by taking advantage of Mxene's high electrical conductivity and large specific surface area (Figure 5f). Owing to the large specific surface area of MXene, Cu-MOF was evenly dispersed on the surface, and the metal sites of MXene and Cu-MOF improved the catalytic ability of H_2O_2 . The electrochemical tests showed that Cu-MOF/Mxene/GCE had a wide linear range of 1 μ M to 6.12 mM at -0.35 V with a detection limit of 0.35 μ M. The material was also used to measure H_2O_2 in milk and serum with good recovery.

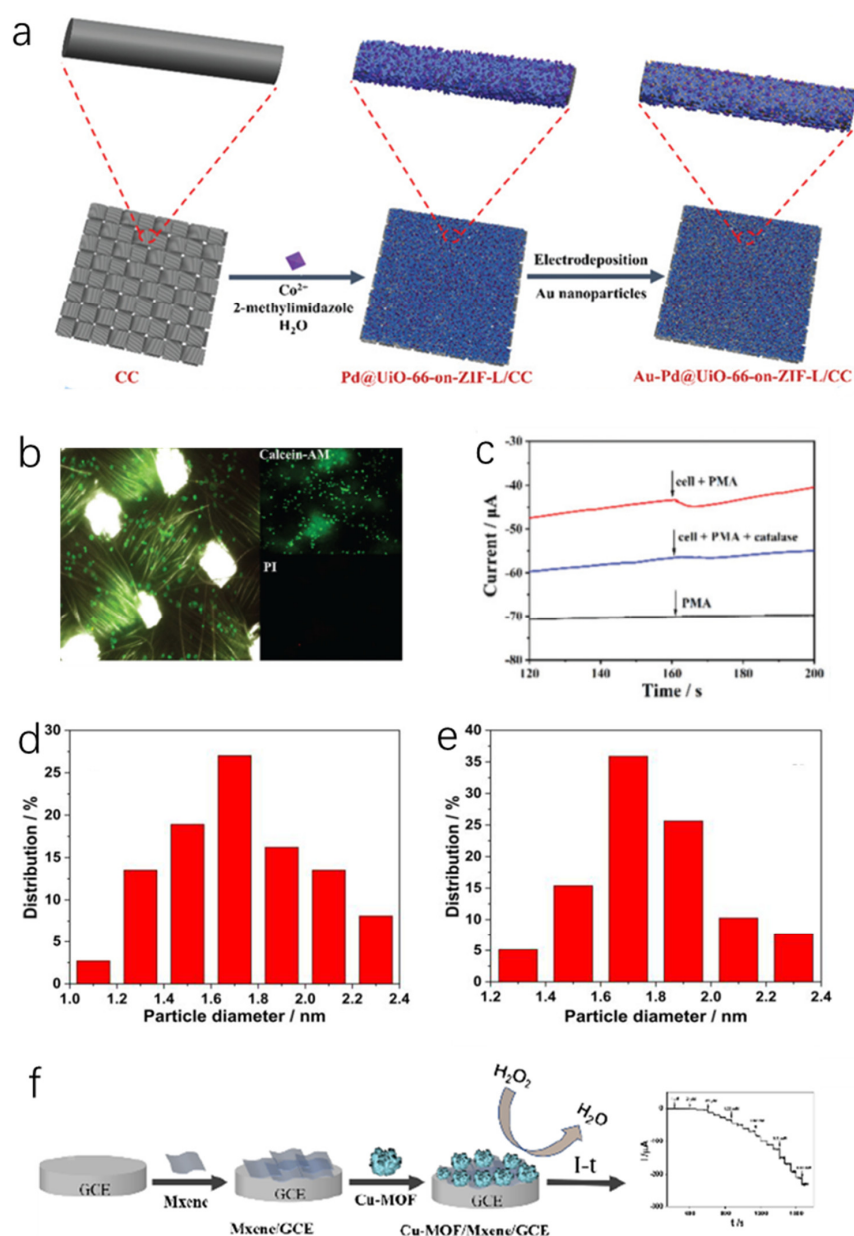


Figure 5. (a) Schematic diagram of the synthesis of Au-Pd@UiO-66-on-ZIF-L on CC; (b) Fluorescence spectra of A549 cells grown on Au-Pd@UiO-66-on-ZIF-L/CC stained by Calcein-AM (green) and PI (red); (c) Amperometric responses of the Au-Pd@UiO-66-on-ZIF-L/CC electrode to H_2O_2 secreted from living A549 cells under drug stimulation at 0.6 V [67]; Copyright 2021, Royal Society of Chemistry. (d) Particle size distributions of AgNPs in AgNPs@Y-1,4-NDC-MOF/ERGO and (e) CuNPs in CuNPs@Y-1,4-NDC-MOF/ERGO [62]; Copyright 2018, Elsevier. (f) The fabrication of the electrochemical sensor for the detection of H_2O_2 [64]. Copyright 2021, Wiley.

4.4. MOF Derivatives Based H_2O_2 Sensor

MOFs are often treated as self-sacrificing metal-organic precursors by post-treatment or high-temperature pyrolysis to construct well-defined heteroatom-doped carbonaceous microstructures with specific surface properties. A variety of typical 3D MOFs such as Prussian Blue, MOF-5, ZIF-67, and HKUST (Hong Kong university of science and technology, also called MOF-199)-1 are widely used as precursors or templates to build novel energy storage structures [135–140]. Furthermore, it has been reported that the carbon hybridization of transition metal oxides can not only improve the electrical conductivity of the catalyst, but also effectively prevent the aggregation of the catalyst. Therefore, transition

metal oxides are often used as precursors for MOF derivatives [141–143]. Firstly, transition metal oxides are often used to provide active sites for enzyme-free detection and improve the activity of catalysts. Secondly, in situ formed CNT framework can improve the electronic conductivity, which is beneficial to the mass transfer of target molecules. Thirdly, the encapsulated carbon shell can effectively immobilize the oxidized nanoparticles, thereby inhibiting their aggregation. Qin's [144] group successfully pyrolyzed the MOFs and fabricated hollow frameworks of Co_3O_4 /n-doped carbon nanotubes (Co_3O_4 /NCNTs) in air. It indicated that Co_3O_4 nanoparticles supplied active sites for the enzyme-free detection of H_2O_2 , and the in situ formed carbon nanotube framework enhanced the electronic conductivity and accelerated the mass transfer of target molecules (Figure 6a). The encapsulated carbon shell could potentially immobilize the oxidized nanoparticles, thus inhibiting their aggregation (Figure 6b). The established hollow frameworks exhibited excellent bifunctional detection capability with high sensitivity and low detection limitation for H_2O_2 ($87.40 \mu\text{A} (\text{mmol/L})^{-1} \text{cm}^{-2}$, 1 mmol/L) and glucose (5 mmol/L) (Figure 6c). This provides an effective idea for the establishment of non-enzymatic sensors with multifunctional detection for biological applications. In addition to the Co_3O_4 /NCNTs hollow frameworks, Cui et al. [145] successfully synthesized hollow mesoporous CuCo_2O_4 (meso- CuCo_2O_4) microspheres and utilized them in both H_2O_2 sensors and glucose biofuel cells (GFCs) for the first time (Figure 6d,e). Meanwhile, the nitrogen adsorption-desorption isotherm of meso- CuCo_2O_4 was a type IV isotherm, confirming the existence of mesoporous structure and the intrinsic high specific surface area. On this basis, the inherently high catalytic activity of mesoporous CuCo_2O_4 exhibits high sensitivity and low detection limit (3 nM) for H_2O_2 (Figure 6f). This further demonstrates that tunable porous structure can be constructed through MOFs template sacrificial method. Meanwhile, more metals active sites can be loaded with the increased surface area. It should be noted is that the calcination temperature needs to be precisely controlled, in order to prevent the potential issues of agglomeration and resulting reduced catalytic activity.

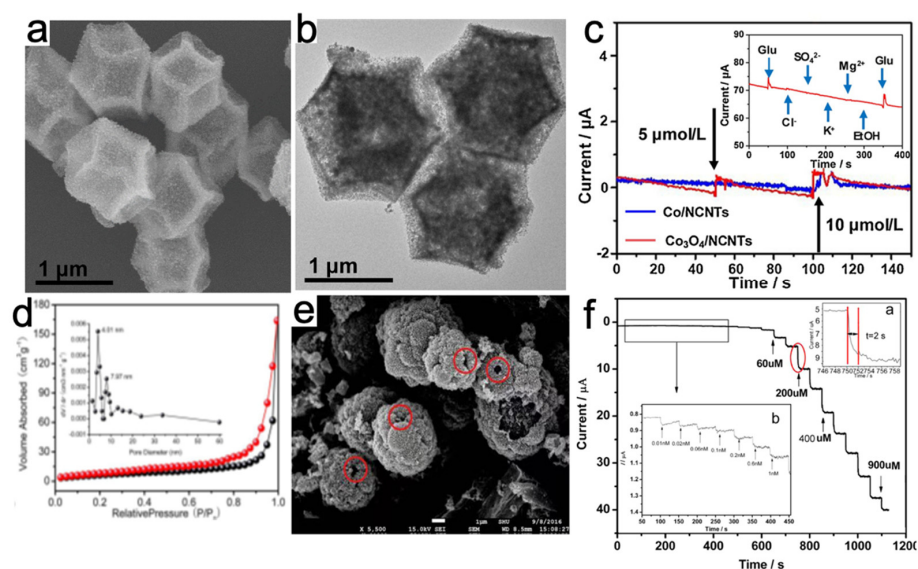


Figure 6. (a) Typical SEM images of Co_3O_4 /NCNTs; (b) Typical TEM images of Co_3O_4 /NCNTs; (c) Amperometric responses of Co/NCNTs and Co_3O_4 /NCNTs with the addition of the same concentration H_2O_2 [144]; Copyright 2020, Elsevier. (d) Nitrogen adsorption-desorption isotherm of meso- CuCo_2O_4 . Insets, respectively, show the crystal structure and distribution of pore size of meso- CuCo_2O_4 ; (e) SEM image of meso- CuCo_2O_4 ; (f) Current-time curve of different H_2O_2 concentrations on CuCo_2O_4 /CPE in 0.2 M NaOH electrolyte at $+0.5 \text{ V}$. Insets a and b respectively were response time of addition H_2O_2 and current-time curve for a low concentration H_2O_2 [145]. Copyright 2018, Elsevier.

5. Conclusions and Outlook

In summary, we listed the advantages and disadvantages (such as conductivity, catalytic activity, stability, selectivity cost and environmental friendliness) of conducting MOFs, chemically modified MOFs, MOFs composites and MOF derivatives (Figure 7). We consider that the ideal electrochemical sensors for H_2O_2 need to have the features of high conductivity, excellent catalytic activity, high selectivity, long-time stability, low cost, and environmental friendliness.

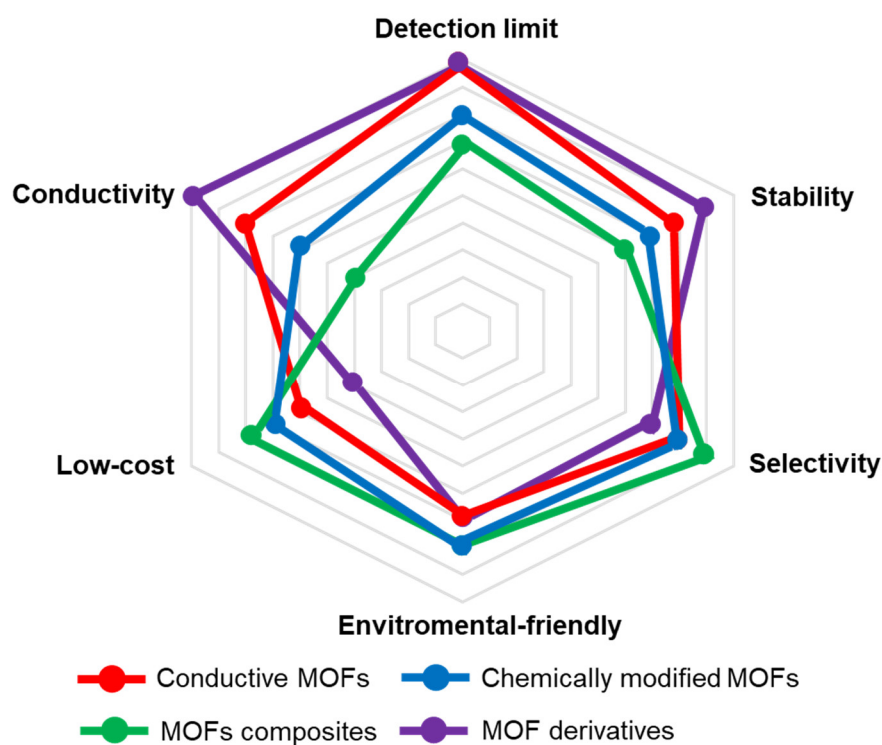


Figure 7. The pros and cons (such as detection limit, conductivity, stability, selectivity, low-cost and environmental-friendly) of the introduced catalysts for H_2O_2 electrochemical sensor (The outside is better, the inside is worse).

(i) Ultra-low detection limit

In order to reduce the detection limit of the sensor, it will be crucial to improve the electrocatalytic activity of the catalyst. Correspondingly, the following strategies can be adopted to improve it: a. Constructing a hollow porous structure not only helps to increase the specific surface area to expose more active sites, but also gives more 3D electron transfer channels; b. Establishing a conductive network improves the conductivity of the catalyst and facilitates electron transfer; c. Composite strategy of coalescing conductive materials or materials with high activity for the decomposition of H_2O_2 enhances conductivity and catalytic activity.

(ii) Long-term stability

It remains a huge challenge to achieve the long-term monitoring of H_2O_2 with sensors without any decrease in activity. In general, catalyzing over a long period of time can lead to the structural changes of materials and deactivation of catalytic sites. To solve this problem, catalysts can be grown directly on highly corrosion-resistant conductive substrates (such as GR nanosheets, conductive glass, Ni foam, etc.)

(iii) Large-scale production

Large-scale production of cheap and efficient H_2O_2 electrochemical sensors is of great significance for practical applications. However, the development process from basic

research to commercialization is seriously hindered by the high price of some raw materials, synthesis processes and few synthesis methods. Therefore, new synthesis methods such as electrospinning, spray drying and Langmuir-Blodgett are needed to achieve precise control and mass production of electrocatalysts.

Overall, the development of highly sensitive and tolerant electrochemical sensors for H₂O₂ is an important and challenging topic in the field of detection. Even in the near future biological enzymes are also currently the best choice for detecting H₂O₂, but this is beyond the scope of this review. We hope that this review can provide some meaningful inspirations for the design and fabrication of MOFs based H₂O₂ electrochemical sensors. It is no doubt that the development of H₂O₂ electrochemical sensors with comprehensive performance and low cost will make significant contributions and breakthroughs in biological, medical and other fields.

Author Contributions: Conceptualization, S.W. and T.Z.; writing—original draft preparation, T.Z. and S.W.; formal analysis, X.Z. and S.Z.; data curation, Z.X. and X.L.; writing—review and editing, M.Z.; supervision, M.Z., Y.J. and L.S.; funding acquisition, M.Z., Y.J. and L.S. All authors have read and agreed to the published version of the manuscript.

Funding: This work was funded by grants from the Natural Science Foundation of China (21401107), the Natural Science Foundation of Jiangsu Province (BK20140986, BK20210650, BK20210651) and The Natural Science Foundation of the Jiangsu Higher Education Institutions of China (21KJB430003). Yachao Jin and Li Song were supported by the Startup Foundation for Introducing Talent of NUIST (2021r047). Meanwhile, this work was supported by Jiangsu Cyan Engineering of Higher Education, Priority Academic Program Development of Jiangsu Higher Education Institutions (PAPD), Jiangsu Joint Laboratory of Atmospheric Pollution Control, and Jiangsu Engineering Technology Research Center of Environmental Cleaning Materials.

Institutional Review Board Statement: Not applicable.

Informed Consent Statement: Not applicable.

Data Availability Statement: Not applicable.

Conflicts of Interest: The authors declare no conflict of interest.

References

1. Salimi, A.; Hallaj, R.; Soltanian, S.; Mamkhezri, H. Nanomolar Detection of Hydrogen Peroxide on Glassy Carbon Electrode Modified with Electrodeposited Cobalt Oxide Nanoparticles. *Anal. Chim. Acta* **2007**, *594*, 24–31. [[CrossRef](#)] [[PubMed](#)]
2. Zhang, M.; Wang, G.; Zheng, B.; Li, L.; Lv, B.; Cao, H.; Chen, M. 3-Layer Conductive Metal-Organic Nanosheets as Electrocatalysts to Enable an Ultralow Detection Limit of H₂O₂. *Nanoscale* **2019**, *11*, 5058–5063. [[CrossRef](#)] [[PubMed](#)]
3. Mohammed, I.; Nemaikal, M.; Sajjan, V.A.; Puttappashetty, D.B.; Sannegowda, L.K. Electropolymerized Film of Cobalt Tetrabenzimidazolephthalocyanine for the Amperometric Detection of H₂O₂. *J. Electroanal. Chem.* **2018**, *826*, 96–103. [[CrossRef](#)]
4. Chen, W.; Cai, S.; Ren, Q.Q.; Wen, W.; Zhao, Y. Di Recent Advances in Electrochemical Sensing for Hydrogen Peroxide: A Review. *Analyst* **2012**, *137*, 49–58. [[CrossRef](#)] [[PubMed](#)]
5. Izu, K.; Yamamoto, O.; Asahi, M. Occupational Skin Injury by Hydrogen Peroxide. *Dermatology* **2000**, *201*, 61–64. [[CrossRef](#)]
6. SCHRECK, A. Investigation of the Explosive Hazard of Mixtures Containing Hydrogen Peroxide and Different Alcohols. *J. Hazard. Mater.* **2004**, *108*, 1–7. [[CrossRef](#)]
7. Mou, K.; Pan, W.; Han, D.A.N.; Wen, X.I.N.; Cao, F.; Miao, Y.I.; Li, P.A.N. Glycyrrhizin Protects Human Melanocytes from H₂O₂—Induced Oxidative Damage via the Nrf2—Dependent Induction of HO - 1. *Int. J. Mol. Med.* **2019**, *44*, 253–261. [[CrossRef](#)]
8. Li, H.; Xin, C.; Zhang, G.; Han, X.; Qin, W.; Zhang, C.W.; Yu, C.; Jing, S.; Li, L.; Huang, W. A Mitochondria-Targeted Two-Photon Fluorogenic Probe for the Dual-Imaging of Viscosity and H₂O₂ Levels in Parkinson’s Disease Models. *J. Mater. Chem. B* **2019**, *7*, 4243–4251. [[CrossRef](#)]
9. Shu, Y.; Chen, J.; Xu, Z.; Jin, D.; Xu, Q.; Hu, X. Nickel Metal-Organic Framework Nanosheet/Hemin Composite as Biomimetic Peroxidase for Electrocatalytic Reduction of H₂O₂. *J. Electroanal. Chem.* **2019**, *845*, 137–143. [[CrossRef](#)]
10. Gimeno, M.P.; Mayoral, M.C.; Andrés, J.M. A Potentiometric Titration for H₂O₂ Determination in the Presence of Organic Compounds. *Anal. Methods* **2013**, *5*, 1510–1514. [[CrossRef](#)]
11. Hu, H.-C.; Jin, H.-J.; Chai, X.-S. Rapid Determination of Hydrogen Peroxide in Pulp Bleaching Effluents by Headspace Gas Chromatography. *J. Chromatogr. A* **2012**, *1235*, 182–184. [[CrossRef](#)] [[PubMed](#)]
12. Ning, D.; Liu, Q.; Wang, Q.; Du, X.-M.; Ruan, W.-J.; Li, Y. Luminescent MOF Nanosheets for Enzyme Assisted Detection of H₂O₂ and Glucose and Activity Assay of Glucose Oxidase. *Sensors Actuators B Chem.* **2019**, *282*, 443–448. [[CrossRef](#)]

13. El-Nagar, G.A.; Sarhan, R.M.; Abouserie, A.; Maticiu, N.; Bargheer, M.; Lauer mann, I.; Roth, C. Efficient 3D-Silver Flower-like Microstructures for Non-Enzymatic Hydrogen Peroxide (H_2O_2) Amperometric Detection. *Sci. Rep.* **2017**, *7*, 12181. [[CrossRef](#)]
14. Ren, H.; Long, Z.; Cui, M.; Shao, K.; Zhou, K.; Ouyang, J.; Na, N. Dual-Functional Nanoparticles for In Situ Sequential Detection and Imaging of ATP and H_2O_2 . *Small* **2016**, *12*, 3920–3924. [[CrossRef](#)] [[PubMed](#)]
15. Yang, Z.; Zhang, S.; Fu, Y.; Zheng, X.; Zheng, J. Shape-Controlled Synthesis of $CuCo_2S_4$ as Highly-Efficient Electrocatalyst for Nonenzymatic Detection of H_2O_2 . *Electrochim. Acta* **2017**, *255*, 23–30. [[CrossRef](#)]
16. Miah, M.R.; Ohsaka, T. Cathodic Detection of H_2O_2 Using Iodide-Modified Gold Electrode in Alkaline Media. *Anal. Chem.* **2006**, *78*, 1200–1205. [[CrossRef](#)] [[PubMed](#)]
17. Wen, D.; Liu, Q.; Cui, Y.; Yang, H.; Kong, J. TEMPO-Functionalized Nanoporous Au Nanocomposite for the Electrochemical Detection of H_2O_2 . *Int. J. Anal. Chem.* **2018**, *2018*, 1–11. [[CrossRef](#)]
18. Manickam, P.; Vashist, A.; Madhu, S.; Sadasivam, M.; Sakthivel, A.; Kaushik, A.; Nair, M. Gold Nanocubes Embedded Biocompatible Hybrid Hydrogels for Electrochemical Detection of H_2O_2 . *Bioelectrochemistry* **2020**, *131*, 107373. [[CrossRef](#)]
19. Lin, C.Y.; Chang, C.T. Iron Oxide Nanorods Array in Electrochemical Detection of H_2O_2 . *Sensors Actuators B Chem.* **2015**, *220*, 695–704. [[CrossRef](#)]
20. Zhang, X.; Wang, G.; Zhang, W.; Wei, Y.; Fang, B. Fixure-Reduce Method for the Synthesis of Cu_2O /MWCNTs Nanocomposites and Its Application as Enzyme-Free Glucose Sensor. *Biosens. Bioelectron.* **2009**, *24*, 3395–3398. [[CrossRef](#)]
21. Pang, H.; Gao, F.; Lu, Q. Glycine-Assisted Double-Solvothermal Approach for Various Cuprous Oxide Structures with Good Catalytic Activities. *CrystEngComm* **2010**, *12*, 406–412. [[CrossRef](#)]
22. Gao, L.; Zhuang, J.; Nie, L.; Zhang, J.; Zhang, Y.; Gu, N.; Wang, T.; Feng, J.; Yang, D.; Perrett, S.; et al. Intrinsic Peroxidase-like Activity of Ferromagnetic Nanoparticles. *Nat. Nanotechnol.* **2007**, *2*, 577–583. [[CrossRef](#)] [[PubMed](#)]
23. Gopalan, A.I.; Komathi, S.; Sai Anand, G.; Lee, K.P. Nanodiamond Based Sponges with Entrapped Enzyme: A Novel Electrochemical Probe for Hydrogen Peroxide. *Biosens. Bioelectron.* **2013**, *46*, 136–141. [[CrossRef](#)] [[PubMed](#)]
24. Ju, J.; Chen, W. In Situ Growth of Surfactant-Free Gold Nanoparticles on Nitrogen-Doped Graphene Quantum Dots for Electrochemical Detection of Hydrogen Peroxide in Biological Environments. *Anal. Chem.* **2015**, *87*, 1903–1910. [[CrossRef](#)]
25. Peng, M.; Zhao, Y.; Chen, D.; Tan, Y. Free-Standing 3D Electrodes for Electrochemical Detection of Hydrogen Peroxide. *ChemCatChem* **2019**, *11*, 4222–4237. [[CrossRef](#)]
26. Zhang, Y.; Bai, X.; Wang, X.; Shiu, K.K.; Zhu, Y.; Jiang, H. Highly Sensitive Graphene-Pt Nanocomposites Amperometric Biosensor and Its Application in Living Cell H_2O_2 Detection. *Anal. Chem.* **2014**, *86*, 9459–9465. [[CrossRef](#)]
27. Patella, B.; Buscetta, M.; Di Vincenzo, S.; Ferraro, M.; Aiello, G.; Sunseri, C.; Pace, E.; Inguanta, R.; Cipollina, C. Electrochemical Sensor Based on RGO/Au Nanoparticles for Monitoring H_2O_2 Released by Human Macrophages. *Sensors Actuators B Chem.* **2021**, *327*, 128901. [[CrossRef](#)]
28. Kan, M.X.; Wang, X.J.; Zhang, H.M. Detection of H_2O_2 at a Composite Film Modified Electrode with Highly Dispersed Ag Nanoparticles in Nafion. *Chinese Chem. Lett.* **2011**, *22*, 458–460. [[CrossRef](#)]
29. Chou, T.C.; Wu, K.Y.; Hsu, F.X.; Lee, C.K. Pt-MWCNT Modified Carbon Electrode Strip for Rapid and Quantitative Detection of H_2O_2 in Food. *J. Food Drug Anal.* **2018**, *26*, 662–669. [[CrossRef](#)]
30. Niamlaem, M.; Boonyuen, C.; Sangthong, W.; Limtrakul, J.; Zigah, D.; Kuhn, A.; Warakulwit, C. Highly Defective Carbon Nanotubes for Sensitive, Low-Cost and Environmentally Friendly Electrochemical H_2O_2 Sensors: Insight into Carbon Supports. *Carbon N. Y.* **2020**, *170*, 154–164. [[CrossRef](#)]
31. Bao, J.; Yang, H.; Zhao, J.; Yang, C.; Duan, Y.; Lu, W.; Gao, M.; Chen, M.; Huo, D.; Hou, C. In Situ Detection of Released H_2O_2 from Living Cells by Carbon Cloth-Supported Graphene/Au-Pt Nanoparticles. *ACS Appl. Nano Mater.* **2021**, *4*, 9449–9458. [[CrossRef](#)]
32. Wang, H.; Chen, W.; Chen, Q.; Liu, N.; Cheng, H.; Li, T. Metal-Organic Framework (MOF)-Au@Pt Nanoflowers Composite Material for Electrochemical Sensing of H_2O_2 in Living Cells. *J. Electroanal. Chem.* **2021**, *897*, 115603. [[CrossRef](#)]
33. Zong, C.; Li, B.; Wang, J.; Liu, X.; Zhao, W.; Zhang, Q.; Nie, X.; Yu, Y. Visual and Colorimetric Determination of H_2O_2 and Glucose Based on Citrate-Promoted H_2O_2 Sculpturing of Silver Nanoparticles. *Microchim. Acta* **2018**, *185*, 199. [[CrossRef](#)] [[PubMed](#)]
34. Yu, Z.; Li, H.; Zhang, X.X.; Liu, N.; Zhang, X.X. NiO/Graphene Nanocomposite for Determination of H_2O_2 with a Low Detection Limit. *Talanta* **2015**, *144*, 1–5. [[CrossRef](#)] [[PubMed](#)]
35. Chen, S.; Hai, X.; Chen, X.W.; Wang, J.H. In Situ Growth of Silver Nanoparticles on Graphene Quantum Dots for Ultrasensitive Colorimetric Detection of H_2O_2 and Glucose. *Anal. Chem.* **2014**, *86*, 6689–6694. [[CrossRef](#)]
36. Zhang, T.; Zheng, B.; Li, L.; Song, J.; Song, L.; Zhang, M. Fewer-Layer Conductive Metal-Organic Langmuir-Blodgett Films as Electrocatalysts Enable an Ultralow Detection Limit of H_2O_2 . *Appl. Surf. Sci.* **2021**, *539*, 1–6. [[CrossRef](#)]
37. Jiao, L.; Wang, Y.; Jiang, H.L.; Xu, Q. Metal-Organic Frameworks as Platforms for Catalytic Applications. *Adv. Mater.* **2018**, *30*, 1–23. [[CrossRef](#)]
38. Zou, C.; Wu, C. De Functional Porphyrinic Metal-Organic Frameworks: Crystal Engineering and Applications. *Dalt. Trans.* **2012**, *41*, 3879–3888. [[CrossRef](#)]
39. Nath, I.; Chakraborty, J.; Verpoort, F. Metal Organic Frameworks Mimicking Natural Enzymes: A Structural and Functional Analogy. *Chem. Soc. Rev.* **2016**, *45*, 4127–4170. [[CrossRef](#)]
40. Lei, J.; Qian, R.; Ling, P.; Cui, L.; Ju, H. Design and Sensing Applications of Metal-Organic Framework Composites. *TrAC—Trends Anal. Chem.* **2014**, *58*, 71–78. [[CrossRef](#)]

41. Gu, Z.Y.; Park, J.; Raiff, A.; Wei, Z.; Zhou, H.C. Metal-Organic Frameworks as Biomimetic Catalysts. *ChemCatChem* **2014**, *6*, 67–75. [[CrossRef](#)]
42. Gkaniatsou, E.; Sicard, C.; Ricoux, R.; Mahy, J.P.; Steunou, N.; Serre, C. Metal-Organic Frameworks: A Novel Host Platform for Enzymatic Catalysis and Detection. *Mater. Horizons* **2017**, *4*, 55–63. [[CrossRef](#)]
43. Wang, H.S. Metal-Organic Frameworks for Biosensing and Bioimaging Applications. *Coord. Chem. Rev.* **2017**, *349*, 139–155. [[CrossRef](#)]
44. Yi, F.Y.; Chen, D.; Wu, M.K.; Han, L.; Jiang, H.L. Chemical Sensors Based on Metal-Organic Frameworks. *Chempluschem* **2016**, *81*, 675–690. [[CrossRef](#)] [[PubMed](#)]
45. Li, S.; Liu, X.; Chai, H.; Huang, Y. Recent Advances in the Construction and Analytical Applications of Metal-Organic Frameworks-Based Nanozymes. *TrAC Trends Anal. Chem.* **2018**, *105*, 391–403. [[CrossRef](#)]
46. Liu, Y.L.; Zhao, X.J.; Yang, X.X.; Li, Y.F. A Nanosized Metal-Organic Framework of Fe-MIL-88NH₂ as a Novel Peroxidase Mimic Used for Colorimetric Detection of Glucose. *Analyst* **2013**, *138*, 4526–4531. [[CrossRef](#)]
47. Meier, J.; Hofferber, E.; Stapleton, J.A.; Iverson, N.M. Hydrogen Peroxide Sensors for Biomedical Applications. *Chemosensors* **2019**, *7*, 64. [[CrossRef](#)]
48. Gonçalves, J.M.; Martins, P.R.; Rocha, D.P.; Matias, T.A.; Julião, M.S.S.; Munoz, R.A.A.; Angnes, L. Recent Trends and Perspectives in Electrochemical Sensors Based on MOF-Derived Materials. *J. Mater. Chem. C* **2021**, *9*, 8718–8745. [[CrossRef](#)]
49. Zhong, Y.; Li, X.; Chen, J.; Wang, X.; Wei, L.; Fang, L.; Kumar, A.; Zhuang, S.Z.; Liu, J. Recent Advances in MOF-Based Nanoplatfoms Generating Reactive Species for Chemodynamic Therapy. *Dalt. Trans.* **2020**, *49*, 11045–11058. [[CrossRef](#)]
50. Cruz-Navarro, J.A.; Hernandez-Garcia, F.; Alvarez Romero, G.A. Novel Applications of Metal-Organic Frameworks (MOFs) as Redox-Active Materials for Elaboration of Carbon-Based Electrodes with Electroanalytical Uses. *Coord. Chem. Rev.* **2020**, *412*, 213263. [[CrossRef](#)]
51. Kholdeeva, O.; Maksimchuk, N. Metal-Organic Frameworks in Oxidation Catalysis with Hydrogen Peroxide. *Catalysts* **2021**, *11*, 283. [[CrossRef](#)]
52. Zhao, F.; Sun, T.; Geng, F.; Chen, P.; Gao, Y. Metal-Organic Frameworks-Based Electrochemical Sensors and Biosensors. *Int. J. Electrochem. Sci.* **2016**, *14*, 5287–5304. [[CrossRef](#)]
53. Zhang, C.; Wang, M.; Liu, L.; Yang, X.; Xu, X. Electrochemical Investigation of a New Cu-MOF and Its Electrocatalytic Activity towards H₂O₂ Oxidation in Alkaline Solution. *Electrochem. commun.* **2013**, *33*, 131–134. [[CrossRef](#)]
54. Lopa, N.S.; Rahman, M.M.; Ahmed, F.; Chandra Sutradhar, S.; Ryu, T.; Kim, W. A Base-Stable Metal-Organic Framework for Sensitive and Non-Enzymatic Electrochemical Detection of Hydrogen Peroxide. *Electrochim. Acta* **2018**, *274*, 49–56. [[CrossRef](#)]
55. Liu, W.; Pan, H.; Liu, C.; Su, C.; Liu, W.; Wang, K.; Jiang, J. Ultrathin Phthalocyanine-Conjugated Polymer Nanosheet-Based Electrochemical Platform for Accurately Detecting H₂O₂ in Real Time. *ACS Appl. Mater. Interfaces* **2019**, *11*, 11466–11473. [[CrossRef](#)]
56. Xia, L.; Luan, X.; Qu, F.; Lu, L. Co-MOF/Titanium Nanosheet Array: An Excellent Electrocatalyst for Non-Enzymatic Detection of H₂O₂ Released from Living Cells. *J. Electroanal. Chem.* **2020**, *878*, 114553. [[CrossRef](#)]
57. Hu, X.; Huang, Y.; Chen, J.; Zhu, X.; Mao, Z.; Wang, Y.; Hu, R.; Chen, H. MOFs Supported Nanonetworks Hybrid Flower-like Catalysts via Supramolecular-Mediated Cascade Self-Assembly for Sensitive Sensing of H₂O₂. *Sensors Actuators B Chem.* **2021**, *342*, 130076. [[CrossRef](#)]
58. Wang, C.; Zhou, M.; Ma, Y.; Tan, H.; Wang, Y.; Li, Y. Hybridized Polyoxometalate-Based Metal-Organic Framework with Ketjenblack for the Nonenzymatic Detection of H₂O₂. *Chem. An Asian J.* **2018**, *13*, 2054–2059. [[CrossRef](#)]
59. Xing, Y.; Zhang, T.; Lu, N.; Xu, Z.; Song, Y.; Liu, Y.; Liu, M.; Zhao, P.; Zhang, Z.; Yan, X. Catalytic Amplification Based on Hierarchical Heterogeneity Bimetal-Organic Nanostructures with Peroxidase-like Activity. *Anal. Chim. Acta* **2021**, *1173*, 338713. [[CrossRef](#)]
60. Guo, X.; Lin, C.; Zhang, M.; Duan, X.; Dong, X.; Sun, D.; Pan, J.; You, T. 2D/3D Copper-Based Metal-Organic Frameworks for Electrochemical Detection of Hydrogen Peroxide. *Front. Chem.* **2021**, *9*, 1–11. [[CrossRef](#)]
61. Wang, M.Q.; Zhang, Y.; Bao, S.J.; Yu, Y.N.; Ye, C. Ni(II)-Based Metal-Organic Framework Anchored on Carbon Nanotubes for Highly Sensitive Non-Enzymatic Hydrogen Peroxide Sensing. *Electrochim. Acta* **2016**, *190*, 365–370. [[CrossRef](#)]
62. Li, C.; Wu, R.; Zou, J.; Zhang, T.; Zhang, S.; Zhang, Z.; Hu, X.; Yan, Y.; Ling, X. MNPs@anionic MOFs/ERGO with the Size Selectivity for the Electrochemical Determination of H₂O₂ Released from Living Cells. *Biosens. Bioelectron.* **2018**, *116*, 81–88. [[CrossRef](#)] [[PubMed](#)]
63. Li, Y.; Pascal, K.; Jin, X.J. Ni-Mo Modified Metal-Organic Frameworks for High-Performance Supercapacitance and Enzymeless H₂O₂ detection. *CrystEngComm* **2020**, *22*, 5145–5161. [[CrossRef](#)]
64. Cheng, D.; Li, P.; Zhu, X.; Liu, M.; Zhang, Y.; Liu, Y. Enzyme-Free Electrochemical Detection of Hydrogen Peroxide Based on the Three-Dimensional Flower-like Cu-Based Metal Organic Frameworks and MXene Nanosheets[†]. *Chinese J. Chem.* **2021**, *39*, 2181–2187. [[CrossRef](#)]
65. Qiao, X.; Arsalan, M.; Ma, X.; Wang, Y.; Yang, S.; Wang, Y.; Sheng, Q.; Yue, T. A Hybrid of Ultrathin Metal-Organic Framework Sheet and Ultrasmall Copper Nanoparticles for Detection of Hydrogen Peroxide with Enhanced Activity. *Anal. Bioanal. Chem.* **2021**, *413*, 839–851. [[CrossRef](#)] [[PubMed](#)]

66. Nabi, S.; Sofi, F.A.; Rashid, N.; Ingole, P.P.; Bhat, M.A. Metal-Organic Framework Functionalized Sulphur Doped Graphene: A Promising Platform for Selective and Sensitive Electrochemical Sensing of Acetaminophen, Dopamine and H₂O₂. *New J. Chem.* **2022**, *46*, 1588–1600. [[CrossRef](#)]
67. Zheng, J.; Zhao, P.; Zhou, S.; Chen, S.; Liang, Y.; Tian, F.; Zhou, J.; Huo, D.; Hou, C. Development of Au-Pd@UiO-66-on-ZIF-L/CC as a Self-Supported Electrochemical Sensor for: In Situ Monitoring of Cellular Hydrogen Peroxide. *J. Mater. Chem. B* **2021**, *9*, 9031–9040. [[CrossRef](#)]
68. Li, J.; Liu, Z.X.; Li, Y.X.; Shu, G.; Zhang, X.J.; Marks, R.S.; Shan, D. 2-Methylimidazole-Assisted Morphology Modulation of a Copper-Based Metal-Organic Framework Transducer for Enhanced Electrochemical Peroxidase-like Activity. *Electroanalysis* **2021**, *1–8*. [[CrossRef](#)]
69. Liu, X.; Luo, C.; Wu, J.; He, N.; Yu, R.; Liu, X. Construction of a Non-Enzymatic Electrochemical Sensor Based on Metal-Organic-Framework-Derived Manganese Oxide Microspheres for the Detection of Hydrogen Peroxide. *ChemElectroChem* **2021**, *8*, 4141–4147. [[CrossRef](#)]
70. Kim, S.E.; Muthurasu, A. Highly Oriented Nitrogen-Doped Carbon Nanotube Integrated Bimetallic Cobalt Copper Organic Framework for Non-Enzymatic Electrochemical Glucose and Hydrogen Peroxide Sensor. *Electroanalysis* **2021**, *33*, 1333–1345. [[CrossRef](#)]
71. Mathew, G.; Daniel, M.; Peramaiah, K.; Ganesh, M.-R.; Neppolian, B. Real-Time Electrochemical Quantification of H₂O₂ in Living Cancer Cells Using Bismuth Based MOF. *J. Electroanal. Chem.* **2022**, *914*, 116255. [[CrossRef](#)]
72. Zhang, T.; Xing, Y.; Song, Y.; Gu, Y.; Yan, X.; Lu, N.; Liu, H.; Xu, Z.; Xu, H.; Zhang, Z.; et al. AuPt/MOF-Graphene: A Synergistic Catalyst with Surprisingly High Peroxidase-like Activity and Its Application for H₂O₂ Detection. *Anal. Chem.* **2019**, *91*, 10589–10595. [[CrossRef](#)]
73. Wu, Z.; Sun, L.P.; Zhou, Z.; Li, Q.; Huo, L.H.; Zhao, H. Efficient Nonenzymatic H₂O₂ Biosensor Based on ZIF-67 MOF Derived Co Nanoparticles Embedded N-Doped Mesoporous Carbon Composites. *Sensors Actuators B Chem.* **2018**, *276*, 142–149. [[CrossRef](#)]
74. Salman, F.; Zengin, A.; Çelik Kazici, H. Synthesis and Characterization of Fe₃O₄-Supported Metal–Organic Framework MIL-101(Fe) for a Highly Selective and Sensitive Hydrogen Peroxide Electrochemical Sensor. *Ionics (Kiel)*. **2020**, *26*, 5221–5232. [[CrossRef](#)]
75. Hu, Y.; Bai, C.; Li, M.; Hojamberdiev, M.; Geng, D.; Li, X. Tailoring Atomically Dispersed Cobalt-Nitrogen Active Sites in Wrinkled Carbon Nanosheets: Via “Fence” Isolation for Highly Sensitive Detection of Hydrogen Peroxide. *J. Mater. Chem. A* **2022**, *10*, 3190–3200. [[CrossRef](#)]
76. Zhou, S.; Wang, X.; Zhao, P.; Zheng, J.; Yang, M.; Huo, D.; Hou, C. ZIF-67 MOF-Derived Co Nanoparticles Supported on N-Doped Carbon Skeletons for the Amperometric Determination of Hydrogen Peroxide. *Microchim. Acta* **2021**, *188*, 1–10. [[CrossRef](#)] [[PubMed](#)]
77. Xu, L.; Xin, Y.; Ma, Y.; Wang, P. Copper and Molybdenum Dioxide Co-Doped Octahedral Porous Carbon Framework for High Sensitivity Electrochemical Detection of Hydrogen Peroxide. *Ionics (Kiel)*. **2022**, *28*, 919–925. [[CrossRef](#)]
78. Mei, H.; Xie, J.; Li, Z.; Lou, C.; Lei, G.; Liu, X.; Zhang, J. Rational Design of ZnO@ZIF-8 Nanoarrays for Improved Electrochemical Detection of H₂O₂. *CrystEngComm* **2022**, *24*, 1645–1654. [[CrossRef](#)]
79. Xiong, L.; Zhang, Y.; Wu, S.; Chen, F.; Lei, L.; Yu, L.; Li, C. Co₃O₄ Nanoparticles Uniformly Dispersed in Rational Porous Carbon Nano-Boxes for Significantly Enhanced Electrocatalytic Detection of H₂O₂ Released from Living Cells. *Int. J. Mol. Sci.* **2022**, *23*, 3799. [[CrossRef](#)]
80. Park, J.; Lee, M.; Feng, D.; Huang, Z.; Hinckley, A.C.; Yakovenko, A.; Zou, X.; Cui, Y.; Bao, Z. Stabilization of Hexaaminobenzene in a 2D Conductive Metal-Organic Framework for High Power Sodium Storage. *J. Am. Chem. Soc.* **2018**, *140*, 10315–10323. [[CrossRef](#)]
81. Lin, S.S.; Gurol, M.D. Catalytic Decomposition of Hydrogen Peroxide on Iron Oxide: Kinetics, Mechanism, and Implications. *Environ. Sci. Technol.* **1998**, *32*, 1417–1423. [[CrossRef](#)]
82. Ensing, B.; Buda, F.; Baerends, E.J. Fenton-like Chemistry in Water: Oxidation Catalysis by Fe(III) and H₂O₂. *J. Phys. Chem. A* **2003**, *107*, 5722–5731. [[CrossRef](#)]
83. Barb, W.G.; Baxendale, J.H.; George, P.; Hargrave, K.R. Reactions of Ferrous and Ferric Ions with Hydrogen Peroxide. Part II. - The Ferric Ion Reaction. *Trans. Faraday Soc.* **1951**, *47*, 591–616. [[CrossRef](#)]
84. Wiegand, H.L.; Orths, C.T.; Kerpen, K.; Lutze, H.V.; Schmidt, T.C. Investigation of the Iron–Peroxo Complex in the Fenton Reaction: Kinetic Indication, Decay Kinetics, and Hydroxyl Radical Yields. *Environ. Sci. Technol.* **2017**, *51*, 14321–14329. [[CrossRef](#)] [[PubMed](#)]
85. Thakur, B.; Karve, V.V.; Sun, D.T.; Semrau, A.L.; Weiß, L.J.K.; Grob, L.; Fischer, R.A.; Queen, W.L.; Wolfrum, B. An Investigation into the Intrinsic Peroxidase-Like Activity of Fe-MOFs and Fe-MOFs/Polymer Composites. *Adv. Mater. Technol.* **2021**, *6*, 1–9. [[CrossRef](#)]
86. Li, C.; Zhang, L.; Chen, J.; Li, X.; Sun, J.; Zhu, J.; Wang, X.; Fu, Y. Recent Development and Applications of Electrical Conductive MOFs. *Nanoscale* **2021**, *13*, 485–509. [[CrossRef](#)]
87. Li, P.; Wang, B. Recent Development and Application of Conductive MOFs. *Isr. J. Chem.* **2018**, *58*, 1010–1018. [[CrossRef](#)]
88. Contreras-Pereda, N.; Pané, S.; Puigmartí-Luis, J.; Ruiz-Molina, D. Conductive Properties of Triphenylene MOFs and COFs. *Coord. Chem. Rev.* **2022**, *460*. [[CrossRef](#)]

89. Zhu, Y.; Tang, Z. Conductive 2D MOF Coupled with Superprotonic Conduction and Interfacial Pseudo-Capacitance. *Matter* **2020**, *2*, 798–800. [[CrossRef](#)]
90. Shu, Y.; Chen, J.; Xu, Q.; Wei, Z.; Liu, F.; Lu, R.; Xu, S.; Hu, X. MoS₂ Nanosheet–Au Nanorod Hybrids for Highly Sensitive Amperometric Detection of H₂O₂ in Living Cells. *J. Mater. Chem. B* **2017**, *5*, 1446–1453. [[CrossRef](#)]
91. Sarhan, R.M.; El-Nagar, G.A.; Abouserie, A.; Roth, C. Silver–Iron Hierarchical Microflowers for Highly Efficient H₂O₂ Nonenzymatic Amperometric Detection. *ACS Sustain. Chem. Eng.* **2019**, *7*, 4335–4342. [[CrossRef](#)]
92. Chen, D.; Zhuang, X.; Zhai, J.; Zheng, Y.; Lu, H.; Chen, L. Preparation of Highly Sensitive Pt Nanoparticles–Carbon Quantum Dots/Ionic Liquid Functionalized Graphene Oxide Nanocomposites and Application for H₂O₂ Detection. *Sensors Actuators B Chem.* **2018**, *255*, 1500–1506. [[CrossRef](#)]
93. Li, M.; Xu, S.; Tang, M.; Liu, L.; Gao, F.; Wang, Y. Direct Electrochemistry of Horseradish Peroxidase on Graphene-Modified Electrode for Electrocatalytic Reduction towards H₂O₂. *Electrochim. Acta* **2011**, *56*, 1144–1149. [[CrossRef](#)]
94. Bai, G.; Xu, X.; Dai, Q.; Zheng, Q.; Yao, Y.; Liu, S.; Yao, C. An Electrochemical Enzymatic Nanoreactor Based on Dendritic Mesoporous Silica Nanoparticles for Living Cell H₂O₂ Detection. *Analyst* **2019**, *144*, 481–487. [[CrossRef](#)] [[PubMed](#)]
95. Zhang, G.; Jin, L.; Zhang, R.; Bai, Y.; Zhu, R.; Pang, H. Recent Advances in the Development of Electronically and Ionically Conductive Metal–Organic Frameworks. *Coord. Chem. Rev.* **2021**, *439*, 213915. [[CrossRef](#)]
96. Sun, L.; Miyakai, T.; Seki, S.; Dincă, M. Mn²⁺ (2,5-Disulfhydrylbenzene-1,4-Dicarboxylate): A Microporous Metal–Organic Framework with Infinite (–Mn–S–)∞ Chains and High Intrinsic Charge Mobility. *J. Am. Chem. Soc.* **2013**, *135*, 8185–8188. [[CrossRef](#)]
97. Kobayashi, Y.; Jacobs, B.; Allendorf, M.D.; Long, J.R. Conductivity, Doping, and Redox Chemistry of a Microporous Dithiolene-Based Metal–Organic Framework. *Chem. Mater.* **2010**, *22*, 4120–4122. [[CrossRef](#)]
98. Guo, X.; Cao, Q.; Liu, Y.; He, T.; Liu, J.; Huang, S.; Tang, H.; Ma, M. Organic Electrochemical Transistor for in Situ Detection of H₂O₂ Released from Adherent Cells and Its Application in Evaluating the In Vitro Cytotoxicity of Nanomaterial. *Anal. Chem.* **2020**, *92*, 908–915. [[CrossRef](#)]
99. Hu, X.-W.; Mao, C.-J.; Song, J.-M.; Niu, H.-L.; Zhang, S.-Y.; Cui, R.-J. Direct Electrochemistry and Electrocatalytic Behavior of Hemoglobin Entrapped in Ag@C Nanocables/Gold Nanoparticles Nanocomposites Film. *J. Nanosci. Nanotechnol.* **2012**, *12*, 7980–7985. [[CrossRef](#)]
100. Sheberla, D.; Sun, L.; Blood-Forsythe, M.A.; Er, S.; Wade, C.R.; Brozek, C.K.; Aspuru-Guzik, A.; Dincă, M. High Electrical Conductivity in Ni₃(2,3,6,7,10,11-Hexamino-triphenylene)₂, a Semiconducting Metal–Organic Graphene Analogue. *J. Am. Chem. Soc.* **2014**, *136*, 8859–8862. [[CrossRef](#)]
101. Tominaka, S.; Coudert, F.-X.; Dao, T.D.; Nagao, T.; Cheetham, A.K. Insulator-to-Proton-Conductor Transition in a Dense Metal–Organic Framework. *J. Am. Chem. Soc.* **2015**, *137*, 6428–6431. [[CrossRef](#)] [[PubMed](#)]
102. Dong, X.Y.; Hu, X.P.; Yao, H.C.; Zang, S.Q.; Hou, H.W.; Mak, T.C.W. Alkaline Earth Metal (Mg, Sr, Ba)-Organic Frameworks Based on 2,2',6,6'-Tetracarboxybiphenyl for Proton Conduction. *Inorg. Chem.* **2014**, *53*, 12050–12057. [[CrossRef](#)] [[PubMed](#)]
103. Zou, L.; Yao, S.; Zhao, J.; Li, D.S.; Li, G.; Huo, Q.; Liu, Y. Enhancing Proton Conductivity in a 3D Metal–Organic Framework by the Cooperation of Guest [Me₂NH₂]⁺ Cations, Water Molecules, and Host Carboxylates. *Cryst. Growth Des.* **2017**, *17*, 3556–3561. [[CrossRef](#)]
104. Ponomareva, V.G.; Kovalenko, K.A.; Chupakhin, A.P.; Dybtsev, D.N.; Shutova, E.S.; Fedin, V.P. Imparting High Proton Conductivity to a Metal–Organic Framework Material by Controlled Acid Impregnation. *J. Am. Chem. Soc.* **2012**, *134*, 15640–15643. [[CrossRef](#)] [[PubMed](#)]
105. Phang, W.J.; Jo, H.; Lee, W.R.; Song, J.H.; Yoo, K.; Kim, B.; Hong, C.S. Superprotonic Conductivity of a UiO-66 Framework Functionalized with Sulfonic Acid Groups by Facile Postsynthetic Oxidation. *Angew. Chemie Int. Ed.* **2015**, *54*, 5142–5146. [[CrossRef](#)] [[PubMed](#)]
106. Meng, X.; Wei, M.-J.; Wang, H.-N.; Zang, H.-Y.; Zhou, Z.-Y. Multifunctional Luminescent Zn(II)-Based Metal–Organic Framework for High Proton-Conductivity and Detection of Cr³⁺ Ions in the Presence of Mixed Metal Ions. *Dalt. Trans.* **2018**, *47*, 1383–1387. [[CrossRef](#)] [[PubMed](#)]
107. Ding, Y.; Wang, Y.; Lei, Y. Direct Electrochemistry and Electrocatalysis of Novel Single-Walled Carbon Nanotubes–Hemoglobin Composite Microbelts—Towards the Development of Sensitive and Mediator-Free Biosensor. *Biosens. Bioelectron.* **2010**, *26*, 390–397. [[CrossRef](#)] [[PubMed](#)]
108. Wang, G.-X.; Qian, Y.; Cao, X.-X.; Xia, X.-H. Direct Electrochemistry of Cytochrome c on a Graphene/Poly(3,4-Ethylenedioxythiophene) Nanocomposite Modified Electrode. *Electrochem. Commun.* **2012**, *20*, 1–3. [[CrossRef](#)]
109. Sheng, M.; Gao, Y.; Sun, J.; Gao, F. Carbon Nanodots–Chitosan Composite Film: A Platform for Protein Immobilization, Direct Electrochemistry and Bioelectrocatalysis. *Biosens. Bioelectron.* **2014**, *58*, 351–358. [[CrossRef](#)]
110. Lu, C.; Ben, T.; Xu, S.; Qiu, S. Electrochemical Synthesis of a Microporous Conductive Polymer Based on a Metal–Organic Framework Thin Film. *Angew. Chemie Int. Ed.* **2014**, *53*, 6454–6458. [[CrossRef](#)]
111. Qin, X.; Lu, W.; Luo, Y.; Chang, G.; Sun, X. Preparation of Ag Nanoparticle-Decorated Polypyrrole Colloids and Their Application for H₂O₂ Detection. *Electrochem. Commun.* **2011**, *13*, 785–787. [[CrossRef](#)]
112. Chansi; Bhardwaj, R.; Rao, R.P.; Mukherjee, I.; Agrawal, P.K.; Basu, T.; Bharadwaj, L.M. Layered Construction of Nano Immuno-Hybrid Embedded MOF as an Electrochemical Sensor for Rapid Quantification of Total Pesticides Load in Vegetable Extract. *J. Electroanal. Chem.* **2020**, *873*, 114386. [[CrossRef](#)]

113. Usov, P.M.; Ahrenholtz, S.R.; Maza, W.A.; Stratakes, B.; Epley, C.C.; Kessinger, M.C.; Zhu, J.; Morris, A.J. Cooperative Electrochemical Water Oxidation by Zr Nodes and Ni-Porphyrin Linkers of a PCN-224 MOF Thin Film. *J. Mater. Chem. A* **2016**, *4*, 16818–16823. [[CrossRef](#)]
114. Xu, S.; Liu, R.; Shi, X.; Ma, Y.; Hong, M.; Chen, X.; Wang, T.; Li, F.; Hu, N.; Yang, Z. A Dual CoNi MOF Nanosheet/Nanotube Assembled on Carbon Cloth for High Performance Hybrid Supercapacitors. *Electrochim. Acta* **2020**, *342*, 136124. [[CrossRef](#)]
115. Wu, S.; Li, C.; Shi, H.; Huang, Y.; Li, G. Design of Metal-Organic Framework-Based Nanoprobes for Multicolor Detection of DNA Targets with Improved Sensitivity. *Anal. Chem.* **2018**, *90*, 9929–9935. [[CrossRef](#)] [[PubMed](#)]
116. Luo, Y.H.; Chen, C.; He, C.; Zhu, Y.Y.; Hong, D.L.; He, X.T.; An, P.J.; Wu, H.S.; Sun, B.W. Single-Layered Two-Dimensional Metal-Organic Framework Nanosheets as an in Situ Visual Test Paper for Solvents. *ACS Appl. Mater. Interfaces* **2018**, *10*, 28860–28867. [[CrossRef](#)]
117. Yuan, K.; Song, T.; Wang, D.; Zou, Y.; Li, J.; Zhang, X.; Tang, Z.; Hu, W. Bimetal-Organic Frameworks for Functionality Optimization: MnFe-MOF-74 as a Stable and Efficient Catalyst for the Epoxidation of Alkenes with H₂O₂. *Nanoscale* **2018**, *10*, 1591–1597. [[CrossRef](#)]
118. Li, Y.; Cheng, C.; Yang, Y.P.; Dun, X.J.; Gao, J.; Jin, X.J. A Novel Electrochemical Sensor Based on CuO/H-C₃N₄/RGO Nanocomposite for Efficient Electrochemical Sensing Nitrite. *J. Alloys Compd.* **2019**, *798*, 764–772. [[CrossRef](#)]
119. Li, Y.; Cui, L.; Jia, M.; Xu, L.; Gao, J.; Jin, X. Hydrophilic “Bridge” Tannins for Stabilizing the Metal Selenides onto Activated Carbon for Binder-Free and Ultralong-Life Asymmetric Supercapacitors. *New J. Chem.* **2019**, *43*, 5592–5602. [[CrossRef](#)]
120. Li, Y.; Xu, L.; Gao, J.; Jin, X. Hydrothermal Fabrication of Reduced Graphene Oxide/Activated Carbon/MnO₂ Hybrids with Excellent Electrochemical Performance for Supercapacitors. *RSC Adv.* **2017**, *7*, 39024–39033. [[CrossRef](#)]
121. Guo, L.; Wang, J.; Teng, X.; Liu, Y.; He, X.; Chen, Z. A Novel Bimetallic Nickel–Molybdenum Carbide Nanowire Array for Efficient Hydrogen Evolution. *ChemSusChem* **2018**, *11*, 2717–2723. [[CrossRef](#)] [[PubMed](#)]
122. Ai, L.; Li, L.; Zhang, C.; Fu, J.; Jiang, J. MIL-53(Fe): A Metal-Organic Framework with Intrinsic Peroxidase-like Catalytic Activity for Colorimetric Biosensing. *Chem. A Eur. J.* **2013**, *19*, 15105–15108. [[CrossRef](#)] [[PubMed](#)]
123. Valekar, A.H.; Batule, B.S.; Kim, M.I.; Cho, K.H.; Hong, D.Y.; Lee, U.H.; Chang, J.S.; Park, H.G.; Hwang, Y.K. Novel Amine-Functionalized Iron Trimesates with Enhanced Peroxidase-like Activity and Their Applications for the Fluorescent Assay of Choline and Acetylcholine. *Biosens. Bioelectron.* **2018**, *100*, 161–168. [[CrossRef](#)] [[PubMed](#)]
124. Zhao, M.; Lu, Q.; Ma, Q.; Zhang, H. Two-Dimensional Metal–Organic Framework Nanosheets. *Small Methods* **2017**, *1*, 1–8. [[CrossRef](#)]
125. Zhao, M.; Huang, Y.; Peng, Y.; Huang, Z.; Ma, Q.; Zhang, H. Two-Dimensional Metal-Organic Framework Nanosheets: Synthesis and Applications. *Chem. Soc. Rev.* **2018**, *47*, 6267–6295. [[CrossRef](#)]
126. Liu, X.; Yan, Z.; Zhang, Y.; Liu, Z.; Sun, Y.; Ren, J.; Qu, X. Two-Dimensional Metal-Organic Framework/Enzyme Hybrid Nanocatalyst as a Benign and Self-Activated Cascade Reagent for in Vivo Wound Healing. *ACS Nano* **2019**, *13*, 5222–5230. [[CrossRef](#)]
127. Cheng, H.; Liu, Y.; Hu, Y.; Ding, Y.; Lin, S.; Cao, W.; Wang, Q.; Wu, J.; Muhammad, F.; Zhao, X.; et al. Monitoring of Heparin Activity in Live Rats Using Metal-Organic Framework Nanosheets as Peroxidase Mimics. *Anal. Chem.* **2017**, *89*, 11552–11559. [[CrossRef](#)]
128. Tang, Y.; Hu, Y.; Yang, Y.; Liu, B.; Wu, Y. A Facile Colorimetric Sensor for Ultrasensitive and Selective Detection of Lead(II) in Environmental and Biological Samples Based on Intrinsic Peroxidase-Mimic Activity of WS₂ Nanosheets. *Anal. Chim. Acta* **2020**, *1106*, 115–125. [[CrossRef](#)]
129. Wang, W.; Zou, Y.; Yan, J.; Liu, J.; Chen, H.; Li, S.; Zhang, L. Ultrasensitive Colorimetric Immunoassay for HCG Detection Based on Dual Catalysis of Au@Pt Core–Shell Nanoparticle Functionalized by Horseradish Peroxidase. *Spectrochim. Acta Part A Mol. Biomol. Spectrosc.* **2018**, *193*, 102–108. [[CrossRef](#)]
130. Das, N. Recovery of Precious Metals through Biosorption - A Review. *Hydrometallurgy* **2010**, *103*, 180–189. [[CrossRef](#)]
131. Xia, Y.; Yang, X. Toward Cost-Effective and Sustainable Use of Precious Metals in Heterogeneous Catalysts. *Acc. Chem. Res.* **2017**, *50*, 450–454. [[CrossRef](#)] [[PubMed](#)]
132. Yu, J.; Mu, C.; Yan, B.; Qin, X.; Shen, C.; Xue, H.; Pang, H. Materials Horizons Nanoparticle/MOF Composites: Preparations and Applications. *Mater. Horizons* **2017**, *4*, 557–569. [[CrossRef](#)]
133. Copéret, C. Synthesis of Solid Catalysts. Edited by Krijn P. de Jong. *ChemCatChem* **2010**, *2*, 706. [[CrossRef](#)]
134. Ding, K.; Cullen, D.A.; Zhang, L.; Cao, Z.; Roy, A.D.; Ivanov, I.N.; Cao, D. A General Synthesis Approach for Supported Bimetallic Nanoparticles via Surface Inorganometallic Chemistry. *Science* **2018**, *362*, 560–564. [[CrossRef](#)] [[PubMed](#)]
135. Wei, T.; Zhang, M.; Wu, P.; Tang, Y.J.; Li, S.L.; Shen, F.C.; Wang, X.L.; Zhou, X.P.; Lan, Y.Q. POM-Based Metal-Organic Framework/Reduced Graphene Oxide Nanocomposites with Hybrid Behavior of Battery-Supercapacitor for Superior Lithium Storage. *Nano Energy* **2017**, *34*, 205–214. [[CrossRef](#)]
136. Xia, W.; Qu, C.; Liang, Z.; Zhao, B.; Dai, S.; Qiu, B.; Jiao, Y.; Zhang, Q.; Huang, X.; Guo, W.; et al. High-Performance Energy Storage and Conversion Materials Derived from a Single Metal-Organic Framework/Graphene Aerogel Composite. *Nano Lett.* **2017**, *17*, 2788–2795. [[CrossRef](#)]
137. Zhang, L.; Wu, H.B.; Lou, X.W. Metal-Organic-Frameworks-Derived General Formation of Hollow Structures with High Complexity. *J. Am. Chem. Soc.* **2013**, *135*, 10664–10672. [[CrossRef](#)]

138. Zou, F.; Hu, X.; Li, Z.; Qie, L.; Hu, C.; Zeng, R.; Jiang, Y.; Huang, Y. MOF-Derived Porous ZnO/ZnFe₂O₄/C Octahedra with Hollow Interiors for High-Rate Lithium-Ion Batteries. *Adv. Mater.* **2014**, *26*, 6622–6628. [[CrossRef](#)]
139. Wang, T.; Kim, H.K.; Liu, Y.; Li, W.; Griffiths, J.T.; Wu, Y.; Laha, S.; Fong, K.D.; Podjaski, F.; Yun, C.; et al. Bottom-up Formation of Carbon-Based Structures with Multilevel Hierarchy from MOF-Guest Polyhedra. *J. Am. Chem. Soc.* **2018**, *140*, 6130–6136. [[CrossRef](#)]
140. Zhou, A.; Guo, R.M.; Zhou, J.; Dou, Y.; Chen, Y.; Li, J.R. Pd@ZIF-67 Derived Recyclable Pd-Based Catalysts with Hierarchical Pores for High-Performance Heck Reaction. *ACS Sustain. Chem. Eng.* **2018**, *6*, 2103–2111. [[CrossRef](#)]
141. Zhang, C.; Li, L.; Ju, J.; Chen, W. Electrochemical Sensor Based on Graphene-Supported Tin Oxide Nanoclusters for Nonenzymatic Detection of Hydrogen Peroxide. *Electrochim. Acta* **2016**, *210*, 181–189. [[CrossRef](#)]
142. Dai, H.; Chen, Y.; Niu, X.; Pan, C.; Chen, H.L.; Chen, X. High-Performance Electrochemical Biosensor for Nonenzymatic H₂O₂ Sensing Based on Au@C-Co₃O₄ Heterostructures. *Biosens. Bioelectron.* **2018**, *118*, 36–43. [[CrossRef](#)] [[PubMed](#)]
143. Feng, X.; Zhang, Y.; Song, J.; Chen, N.; Zhou, J.; Huang, Z.; Ma, Y.; Zhang, L.; Wang, L. MnO₂/Graphene Nanocomposites for Nonenzymatic Electrochemical Detection of Hydrogen Peroxide. *Electroanalysis* **2015**, *27*, 353–359. [[CrossRef](#)]
144. Qin, Y.; Sun, Y.; Li, Y.; Li, C.; Wang, L.; Guo, S. MOF Derived Co₃O₄/N-Doped Carbon Nanotubes Hybrids as Efficient Catalysts for Sensitive Detection of H₂O₂ and Glucose. *Chinese Chem. Lett.* **2020**, *31*, 774–778. [[CrossRef](#)]
145. Cui, S.; Gu, S.; Ding, Y.; Zhang, J.; Zhang, Z.; Hu, Z. Hollow Mesoporous CuCo₂O₄ Microspheres Derived from Metal Organic Framework: A Novel Functional Materials for Simultaneous H₂O₂ Biosensing and Glucose Biofuel Cell. *Talanta* **2018**, *178*, 788–795. [[CrossRef](#)]